ABSTRACT

Design and Synthesis of Vascular Disrupting Agents that Bear the Indole Molecular Framework

Parker M. Korbitz

Director: Dr. Kevin G. Pinney, Ph.D

The discovery of colchicine and combretastatin A-4 (**CA4**), two naturally occurring compounds that inhibit tubulin polymerization, have spurred great interest in small-molecule anticancer agents that interact with the tubulin-microtubule protein system and function as antiproliferative agents. A subset of these analogues target established vasculature feeding tumors and are referred to as vascular disrupting agents (VDAs). It has been discovered that a variety of molecules bearing the indole molecular framework that mimic structural features of colchicine and **CA4** function as potent inhibitors of tubulin polymerization and demonstrate promise as VDAs. The Pinney Research Group (Baylor University) previously designed and synthesized **OXi8006**, an indole-bearing VDA that functions as a powerful inhibitor of tubulin polymerization and demonstrates strong cytotoxicity against a variety of human cancer cell lines. Inspired by these previous studies, a variety of **OXi8006** analogues have been prepared by chemical synthesis and evaluated in preliminary biological studies (carried out through collaboration).

APPROVED BY DIRECTOR OF HONORS THESIS

_____

Dr. Kevin G. Pinney, Department of Chemistry & Biochemistry

APPROVED BY THE HONORS PROGRAM

_____

Dr. Elizabeth Corey, Director

Date:_____

DESIGN AND SYNTHESIS OF VASCULAR DISRUPTING AGENTS THAT BEAR THE INDOLE MOLECULAR FRAMEWORK

A Thesis Submitted to the Faculty of

Baylor University

In Partial Fulfillment of the Requirements for the

Honors Program

By

Parker Korbitz

Waco, Texas

May, 2016

TABLE OF CONTENTS

Acknowledgements

The author is thankful for Dr. Kevin G. Pinney for the opportunity to work in the Pinney Group as well as his assistance and advisement throughout the course of writing this paper. The author is also thankful for Zhe Shi for his leadership, direction, and flexibility within the laboratory.

CHAPTER ONE

Introduction

It is no surprise that cancer is currently at the forefront of medical research. It is estimated that over half of the population will be diagnosed with cancer at some point during their lifetime.[1] One major reason for this extraordinary statistic is the fact that people are simply living longer than they used to. In turn, one's genes are exposed to a higher level of mutagens, elevating the incidence of cancer.[2] This is evident in the fact that over half of individuals diagnosed with cancer are 60 years or older. Another reason cancer rates are increasing is the type of food people are consuming. Due to the amount of processed foods and poor eating habits, obesity is at an all-time high, putting more and more people at a higher risk of developing cancer.[3] In fact, approximately one in three Americans suffer from obesity. However, modern technology has allowed better techniques that screen patients for cancer. For example, it was not possible to screen for breast or prostate cancer in young adults just a few decades ago.[4, 5] Now, many lives have been saved due to technological breakthroughs such as these.

1.1 Microtubule Polymerization

Due to the impact that cancer has had on global health, many different therapeutic techniques have been attempted. One of these techniques aims to target tumor cells while leaving the healthy cells untreated. It is hypothesized that due to rapid proliferation, tumor cells are comprised of a less-developed cytoskeleton when

compared to healthy cells, thus they are more susceptible to microtubule depolymerization.[6, 7] It is well known that cancer cells reproduce more rapidly than healthy cells, thus, one possible therapeutic technique is to focus on the tubulin-microtubule system within endothelial cells that line blood vessels feeding tumor cells.[8]

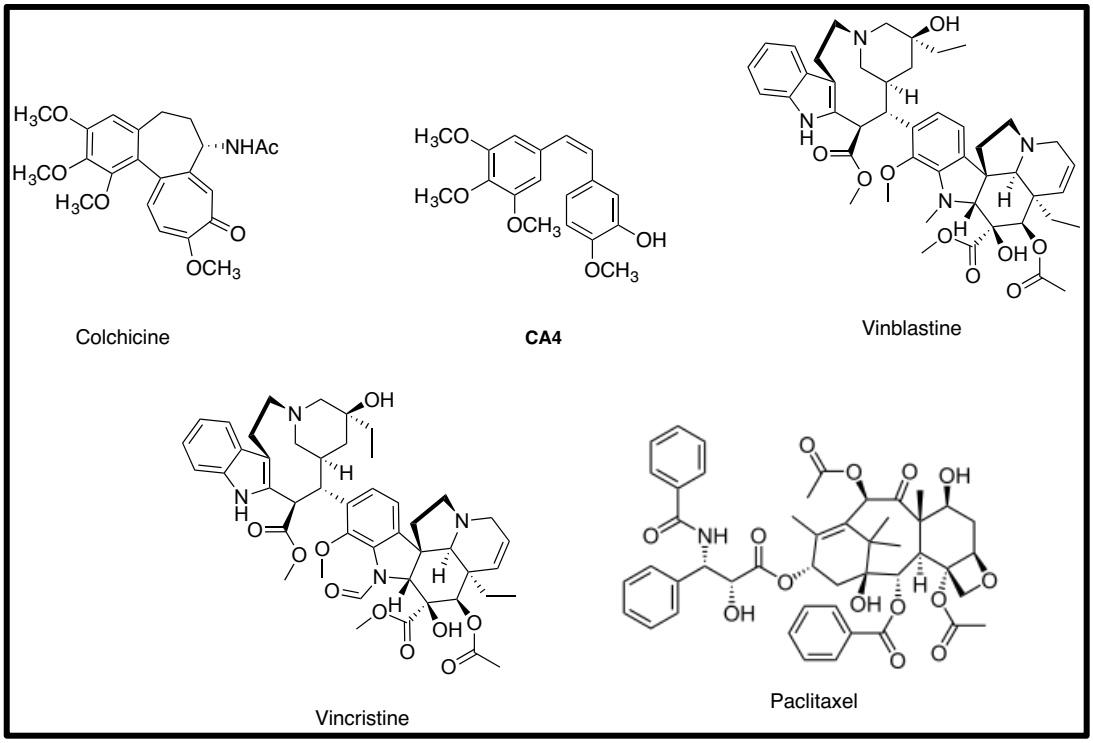

Figure 1. Natural compounds that interact with the tubulin-microtubule protein system[9-12]

Microtubules undergo dynamic instability, which is comprised of a fast shrinking phase and a slower rescue phase when they polymerize. Dynamic instability is a critical component of cell migration, mitotic spindle development, and even chromosomal segregation.[13] Agents that attack this process do so by activating RhoA and other cytoskeletal effectors, leading to a rearrangement within the cytoskeleton.[14,

[15] This change in cytoskeletal structure causes the endothelial cells to change shape, a process known as "blebbing" (Figure 2).[15,16] This morphological change increases the resistance against blood flow, which carry oxygen and nutrients. Eventually, this leads to vascular shutdown, and without adequate vasculature, tumor cells will not receive sufficient amounts of oxygen and nutrients and will ultimately die.

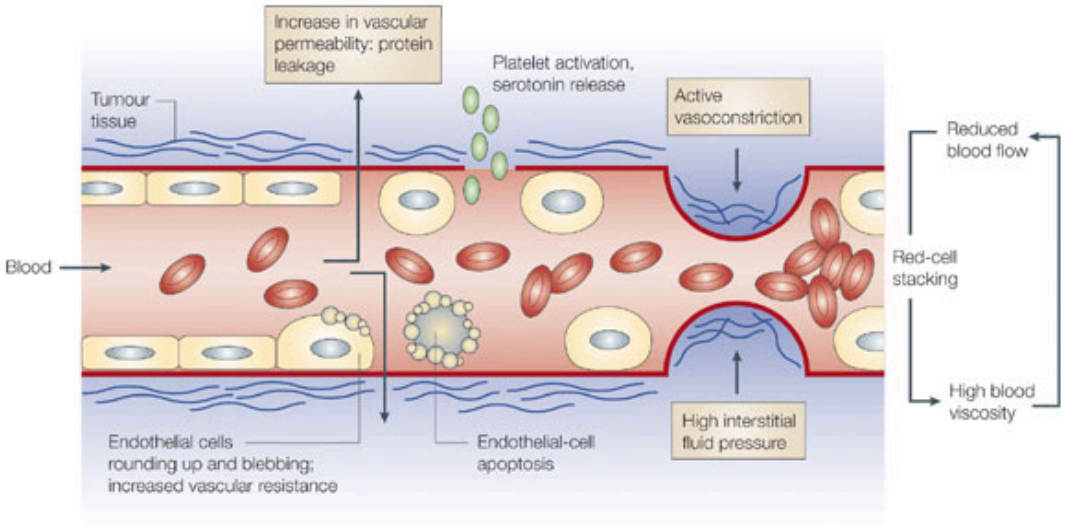

Figure 2. Illustration of VDA mechanism of action[16]

[Reproduced directly from Reference #16]

1.2 Vascular Disrupting Agents

There are two classes of biologically active compounds that do just this. One class comprises angiogenic-inhibiting agents (AIAs) and the other class consists of vascular disrupting agents (VDAs). In both scenarios, the main objective is to deprive the tumor cell of oxygen and nutrients. AIAs intend to stop new blood vessels from forming and are particularly beneficial in patients who are in their early stages of cancer.[17] On the other hand, VDAs target preformed blood vessels and their benefits

are aimed at patients who have cancer in its advanced stages.[18] With the administration of VDAs, endothelial cells of vessels feeding tumors will undergo changes in shape, affecting critical factors essential for survival.[16] The tubulin-microtubule protein system has traditionally been a target for antiproliferative agents.[19] Specifically, various compounds can bind to multiple domains within this system, three of which are the colchicine site, the vinca alkaloid site, and the taxane site. A subset of these compounds, most importantly those that bind to the colchicine site, also function as VDAs.[20]

1.2.1 Colchicine-Binding Domain

The colchicine site is named after one of the first natural compounds that were found to have vascular disrupting properties, colchicine (Figure 3).[9] It was later discovered that the combretastatin family, a naturally-occurring family derived from a South African tree *Combretum caffrum*, contains potent antimitotic agents; most notably combretastatin A-4 (**CA4**) and combretastatin A-1 (**CA1**) (Figure 3).[10, 21] These compounds have been highly investigated as they bind the colchicine-binding site on tubulin. Their corresponding prodrugs, combretastatin A-4 phosphate (**CA4P**) and combretastatin A-1 diphosphate (**CA1P**), have been synthesized in order to alleviate the problems associated with solubility, instability, and cytotoxicity (Figure 3). Specifically, these compounds are inactive derivatives that undergo an enzyme-mediated hydrolysis *in vivo*, resulting in successful release of their active parent drug.[22] Due to the generic 1, 2-diarylethene moiety, these two compounds have been popular in the synthesis of many other derivatives that may be antimitotic agents as

well.[23]

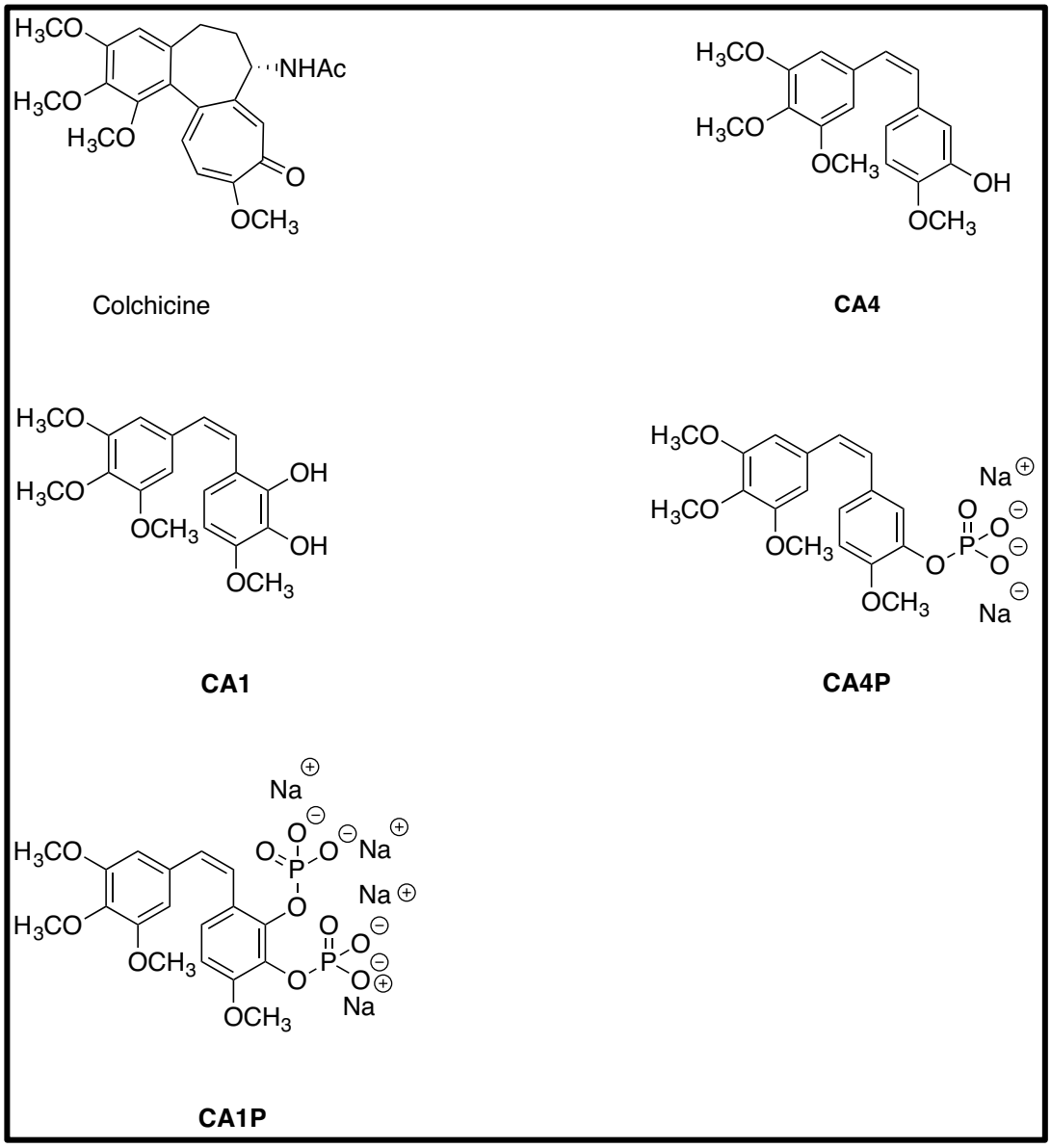

Figure 3. Compounds that bind to the colchicine site[9, 10]

1.2.2 Vinca-Binding Domain

Of the antimitotic agents that bind at the vinca alkaloid site, vincristine and vinblastine were among the first to show strong tubulin polymerization inhibition with an IC_{50} value in the nanomolar concentration.[11] Derived from the leaves of the

Catharanthus roseus plant, these two compounds have been widely studied due to their complex structures, which allow many different analogues to be further investigated (Figure 4). Most notably, urea analogues of vinblastine have even exhibited stronger potencies than vinblastine itself, demonstrating important binding qualities of the vinca alkaloid site.[24] Although the two structures only differ at the N1 position, they have successfully been administered in different types of cancer cells.

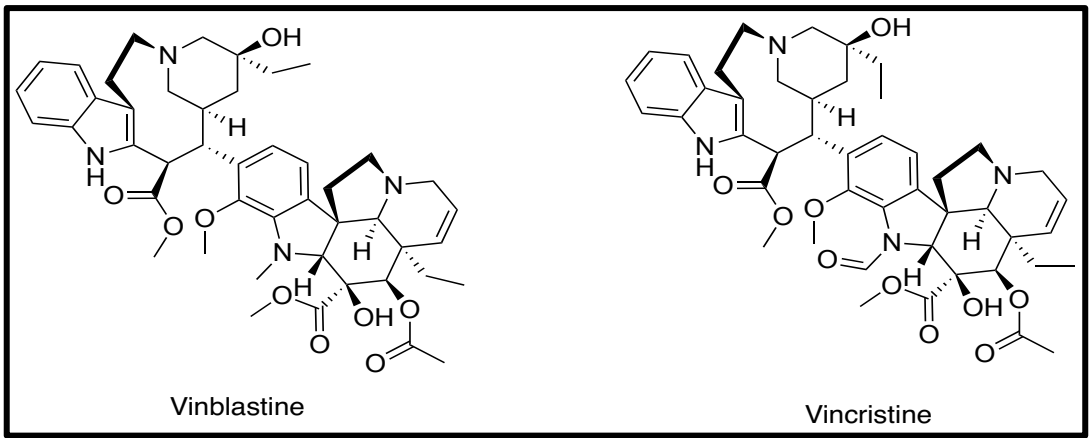

Figure 4. Compounds that bind to the vinca-alkaloid site[11]

1.2.3 Taxoid-Binding Domain

A well-known taxane-binding agent, paclitaxel, is a natural diterpenoid that has been isolated from the *Taxus brevifolia* and has played a major impact in chemotherapeutic therapies.[12] The FDA approved paclitaxel and its synthetic analogue taxotère in the 1990s to treat various types of cancers (Figure 5).[25] These taxane-binding agents accelerate tubulin polymerization and stabilize the mictrotubules, thereby inhibiting microtubule depolymerization, which as discussed earlier, can lead to apoptosis.[26] Taxane-binding agents have been highly studied due to their large molecular structure, thus allowing numerous analogues to be

synthesized and tested for their effects on microtubule depolymerization. What makes taxoids such a critical component of chemotherapy is the fact that these compounds display exceptional potency against multi-drug resistant cancer cell lines.[27] Cancer cells overexpress certain proteins that help remove any cytotoxins from within the cell, thus leading to resistance.[28] However, certain synthetic taxoids have been shown to inhibit these proteins, allowing them to be effective against resistant cancer cell lines.

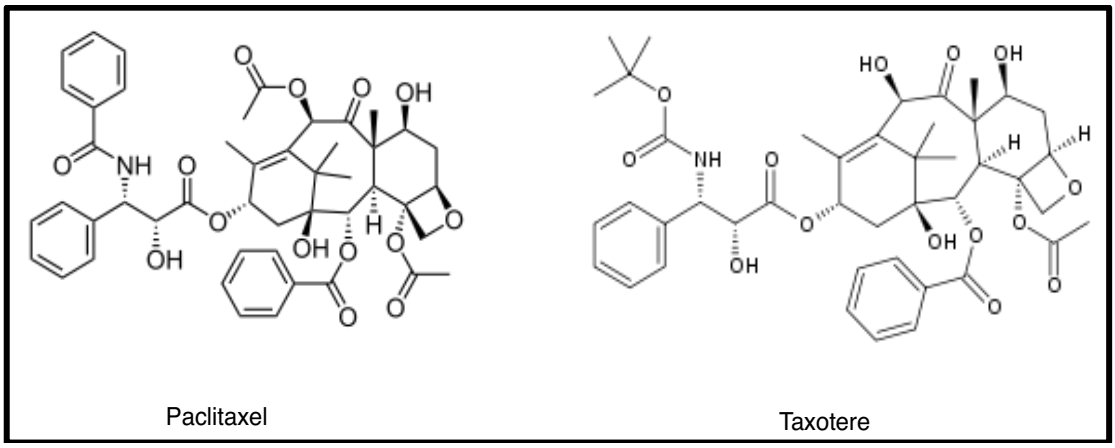

Figure 5. Compounds that bind to the taxane site[12, 25]

1.3 Indole-Based VDAs

The Pinney Research Group (Baylor University) designed and synthesized small-molecule anticancer agents that bear structure resemblance to **CA4** and a variety of corresponding analogues. A host of molecular scaffolds have been developed, including benzo[b]thiophenes, benzo[b]furans, and indoles.[23, 29-33] Most of these molecular frameworks were designed to mimic the *cis*-stillbenoid feature inherent to the combretastatin family as well as preserving the phenolic and 3,4,5-trimethoxyaryl functionalities.[34] **OXi8006** and its phosphate prodrug **OXi8007** are

some of the first indole-based molecules to be evaluated for their ability to inhibit tubulin polymerization, as well as for their cytotoxicity against a select number of cancer cell lines (Figure 6). Based on combretastatin-derived compounds, the indole structure became a well-established molecular framework that is associated with tubulin polymerization inhibition. Structure-Activity Relationship (SAR) studies demonstrate the indole structure's similarity to colchicine, prompting investigation into its ability to inhibit tubulin polymerization.[29] These SAR studies exemplify that an sp^2 center between the two aryl moieties and an unsubstituted N1-position are essential in sustaining strong tubulin polymerization inhibition and reasonable cytotoxicity.[26] Further evaluation demonstrates that **OXi8006** has an IC_{50} value similar to the potent CA4 regarding tubulin binding inhibition as well as comparable GI_{50} values when testing for cytotoxicity against tumor cells. Another CA4 analogue, BPR0L075, is a tubulin-binding agent that exhibits not only *in vitro* but also *in vivo* activity against tumor cells.[35]

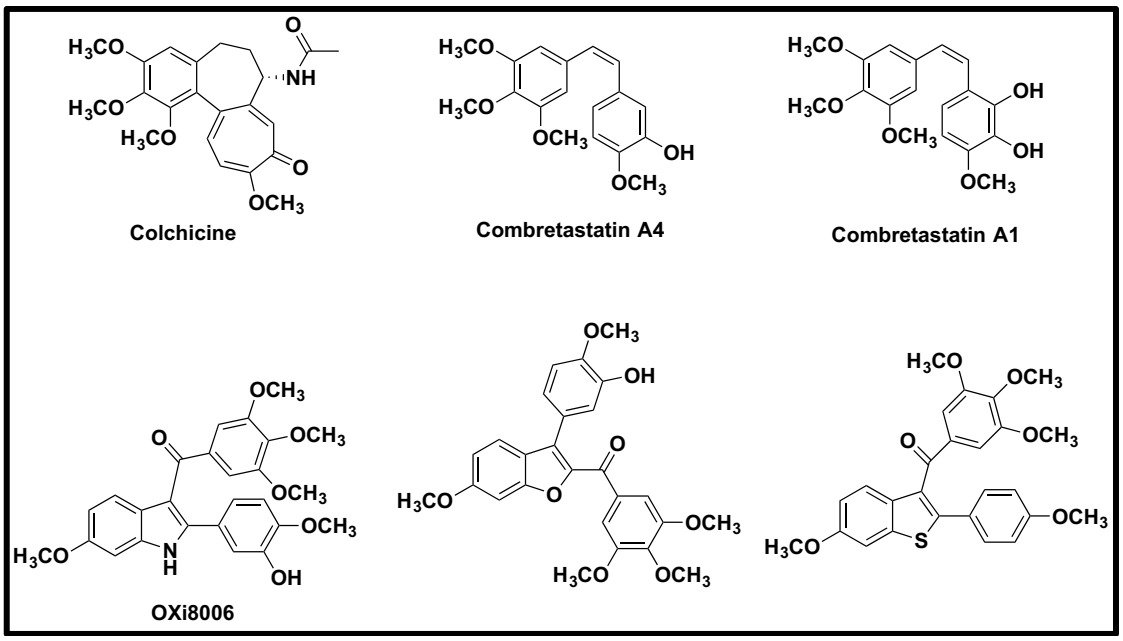

Figure 6. Benzo[*b*]thiophene, benzo[*b*]furan, and indole-based compounds that act as vascular disrupting agents[29, 31, 32, 34]

1.4 Bioreductively Activatable Prodrug Conjugates

As stated earlier, much research has focused on the development of administering VDAs in beneficial, therapeutic means. However, there are a few drawbacks that arise from the use of VDAs. These compounds leave feasible cells at tumor periphery that, when untreated, rapidly divide back into larger tumors. Additionally, some VDA administration methods are too cytotoxic for therapeutic efficacy, which is influenced by two distinct pathways.[36] On the one hand, these drugs can cause vascular shutdown in vessels feeding healthy tissue. On the other hand, they can inhibit cellular proliferation in healthy tissue, resulting in apoptosis. Currently, there is no VDA that has been approved by the FDA for treating individuals who have been diagnosed with cancer, however some are still in clinical

trials (Figure 7).[14] Therefore, new methods are being evaluated in order to remedy some of the problems associated with VDA administration.

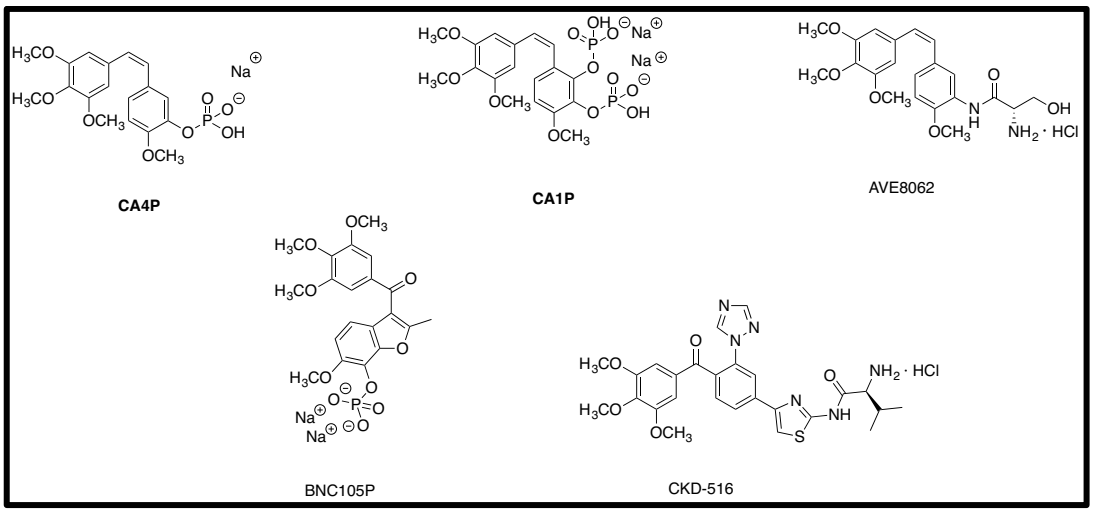

Figure 7. Structures of VDAs that are currently undergoing clinical trials[14]

[Reproduced directly from Reference #14]

One promising technique for administering these VDAs *in vivo* is to use bioreductively activatable prodrug conjugates, otherwise known as BAPCs. One key difference between healthy cells and tumor cells is the distribution of oxygen and nutrients. Healthy tissue is highly organized with an even distribution of oxygen and nutrition whereas malignant tissue is rather chaotic and has defined aerobic regions and hypoxic regions.[37] These hypoxic regions have countless effects on tumor vasculature, which include but are not limited to; increased tumor angiogenesis, vasculogenesis, and metastasis.[38] As a result, these regions are resistant to various chemotherapeutic and radiotherapeutic techniques, prompting investigation for different modes of intervention.[39] BAPCs can be activated only under these hypoxic conditions, as they become reduced by the oxidoreductases present within the tumor,

causing the molecule to undergo a self-cleaving mechanism and release the active drug within the hypoxic environment, displayed in Figure 8. Bioreductive triggers can be attached to various vascular disrupting agents, and only under hypoxic conditions will this mechanism occur.

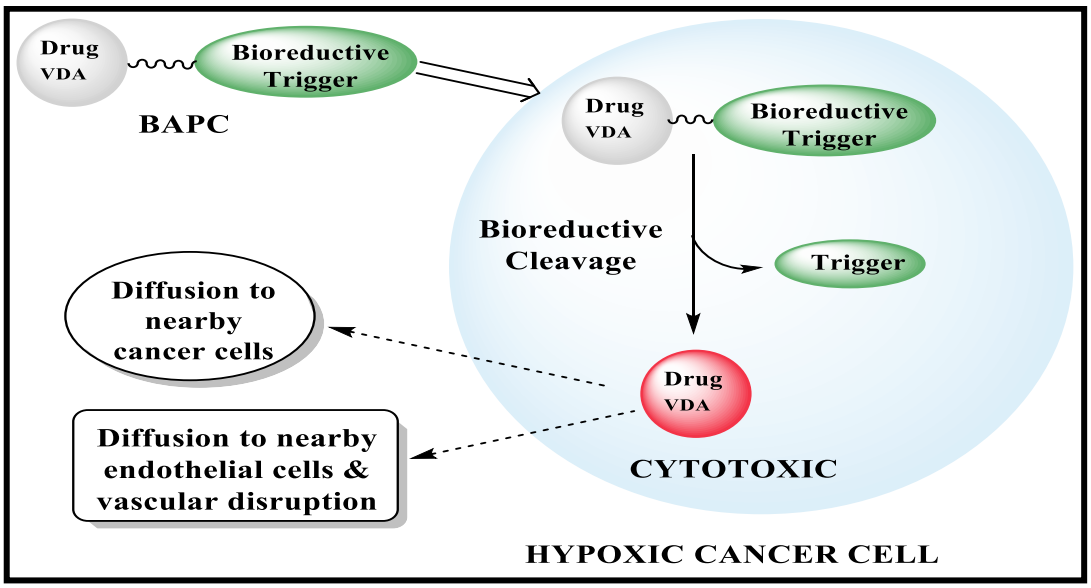

Figure 8. Proposed mechanism for selective release under tumor hypoxia of cytotoxic agent from non-toxic prodrug [40]

There are two BAPCs that are currently undergoing clinical trials (Figure 9). TH-302 is a brominated version of isophosphoramide mustard that, under human cancer cell lines, has exhibited little effect in non-hypoxic conditions but an enhanced potency under hypoxic conditions.[41] When administered at its maximum tolerated dose, TH-302 resulted in 89% tumor growth inhibition and a mere 2.9% loss in body weight. In addition, no significant cytotoxicity values were observed, which was evaluated by changes in white blood cell counts. Another BAPC, PR-104, is reduced

to a nitrogen mustard that induces DNA cross-linking in hypoxic cells.[42] PR-104 exhibited stronger cytotoxic effects under hypoxic than non-hypoxic conditions, however it is activated by the aldo-keto reductase enzyme AKR1C3 under non-hypoxic conditions.[43] It is proposed that this enzyme is at elevated concentrations in certain types of cancers versus healthy tissue. Hypoxia-activated prodrugs have received a lot of attention recently as they provide a means to administer these compounds directly into the hypoxic regions that constitute tumor vasculature.

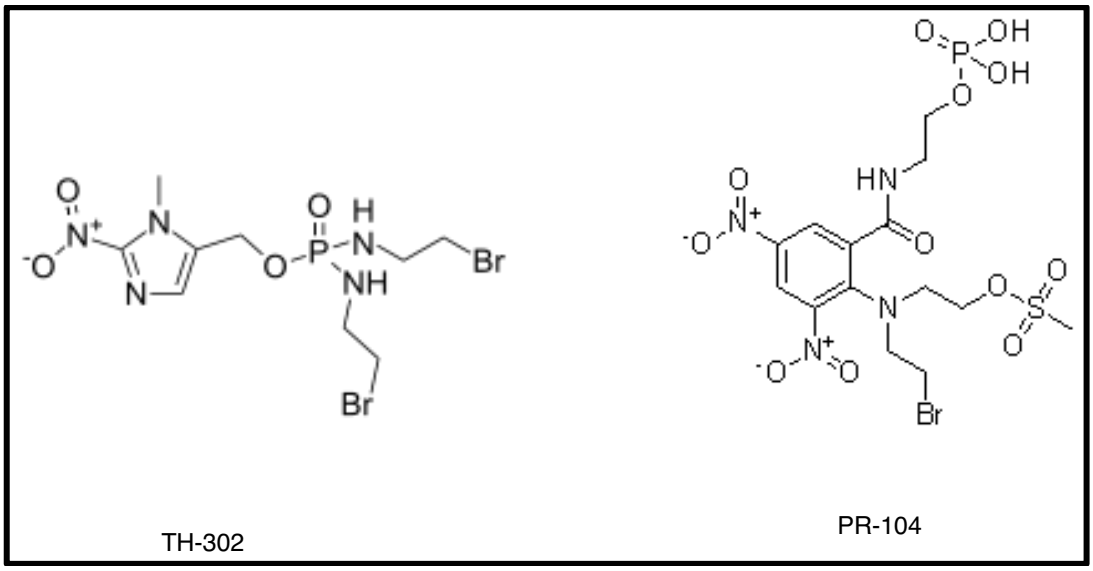

Figure 9. Compounds that act as bioreductively activatable prodrug conjugates[41, 42]

As the indole molecular framework is an important characteristic of some vascular disrupting agents, the objective of this paper is to design and synthesize potential vascular disrupting agents that bear this indole molecular framework. Due to the success that **OXi8006** has had, this paper aims to synthesize the nitro and amino analogues of **OXi8006**, compounds **4** and **5** (Scheme 1).[23, 29, 30] Finally, **OXi8006**,

compound **14** (Scheme 2), will be synthesized in order to have a parent compound that bioreductive triggers will be attached to.

CHAPTER TWO

Results and Discussion

2.1. Chemistry

The commercially available starting material, acetophenone **1**, was brominated (Scheme 1) to afford intermediate **2.** This compound, along with *m*-anisidine, produced the nitro indole **3** via the Bischler Mohlau indole synthesis.[30] The following reaction included the addition of 3,4,5-trimethoxybenzoyl chloride to yield the nitro analogue of **OXi8006**, compound **4**.[44, 45] Reduction via hydrogen gas and palladium on activated carbon afforded the amino analogue of **OXi8006**, compound **5.** [44, 45] The synthesis of **OXi8006** began with protecting the hydroxyl group on the commercially available isovanillin; compound **6**, by *tert*-butyldimethylsilyl chloride (Scheme 2), to form compound **7.** Addition of methyllithium formed the reduced, secondary alcohol **8.** This compound was then oxidized by pyridinium chlorochromate to afford acetophenone **9**. Treatment of LDA solution formed the silyl ether TMS-protected enol ether **10**, which was subsequently brominated to form **11.** Compound **12** was afforded via Bischler-Mohlau indole synthesis, and subsequently, 3, 4, 5-trimethoxybenzoyl chloride was added to produce the TBS-protected indole **13**.[30] Desilylation by TBAF afforded the final compound **14**, otherwise **OXi8006**.

Scheme 1. Synthesis of nitro and amino analogues 4 and 5 of OXi8006

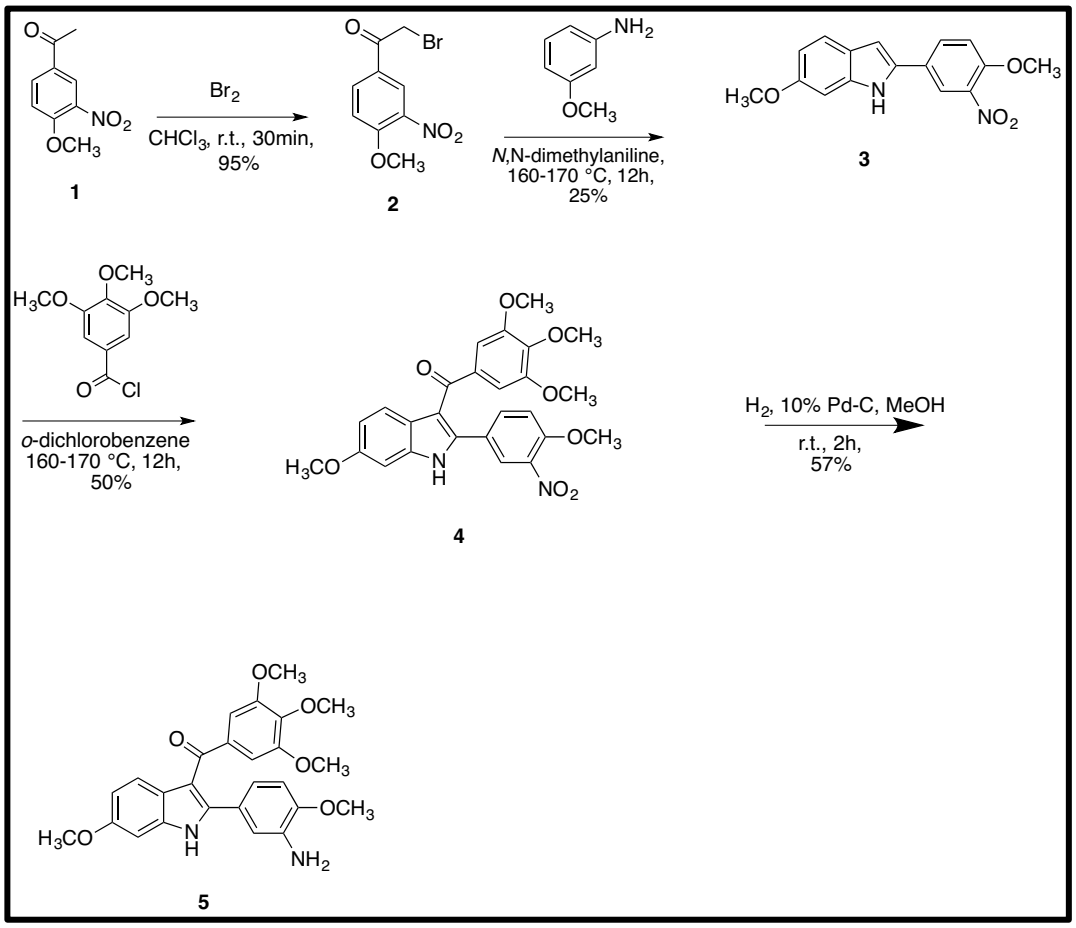

Scheme 2. Synthesis of OXi8006

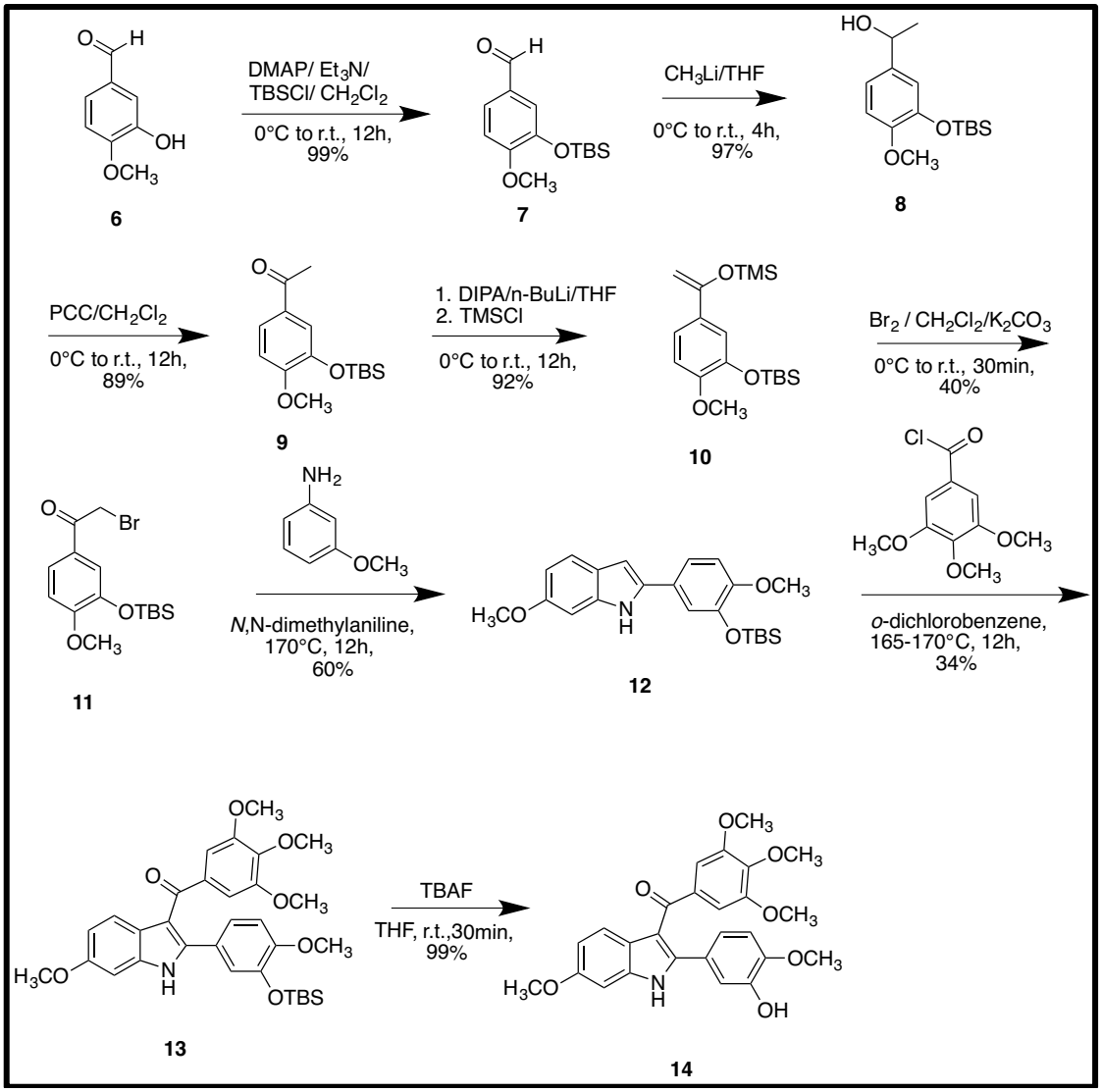

2.2 Biological Evaluation

Compounds **4** and **5** were sent to Dr. Ernest Hamel at the National Institute of Health, who evaluated compound **4** for its cytotoxicity against the MCF-7 cancer cell line and both compounds for their ability to inhibit colchicine binding and tubulin polymerization. The results are displayed below in Table 1.

Table 1. Biological evaluations of Compounds 4 and 5

	MCF-7 Cytotoxicity IC_{50} (nM)	**Inhibition of Colchicine Binding % Inhibition ± SD 5 µM inhibitor**	**Inhibition of Tubulin Polymerization IC_{50} (µM) ± SD**
4	50	40 ± 5	0.97 ± 0.07
5	N/A	59 ± 2	0.83 ± 0.05

CHAPTER THREE

Materials and Methods

3.1 General Experimental Methods:

Dichloromethane, methanol, ethanol, and tetrahydrofuran (THF) were used in their anhydrous forms, as obtained from the chemical suppliers. Reactions were performed under an inert atmosphere using nitrogen gas, unless specified. Thin-layer chromatography (TLC) plates (precoated glass plates with silica gel 60 F254, 0.25 mm thickness) were used to monitor reactions. Purification of intermediates and products was carried out with a Biotage isolera flash purification system using silica gel (200-400 mesh, 60 Å). Intermediates and products synthesized were characterized on the basis of their ^{1}H NMR (600 MHz), ^{13}C NMR (151 MHz), and spectroscopic data using a Bruker Avance III HD 600MHz NMR system. Spectra were recorded in $CDCl_3$. All chemical shifts are expressed in ppm (δ), coupling constants (*J*) are presented in Hz, and peak patterns are reported as broad (br), singlet (s), doublet (d), triplet (t), quartet (q), double doublet, (dd), and multiplet (m). Purity of the final compounds was further analyzed at 25 ^{o}C using an Agilent 1200 HPLC system with a diode-array detector (λ = 190-400 nm), a Zorbax XDB-C18 HPLC column (4.6 mm - 150 mm, 5 μm), and a Zorbax reliance cartridge guard-column; method A: solvent A, acetonitrile, solvent B, H2O; gradient, 10%A / 90%B to 100%A / 0%B over 0 to 40 min; post-time 10 min; flow rate 1.0 mL/min; injection volume 20 μL; monitored at wavelengths of 210, 254, 230, 280, and 360 nm. Mass spectrometry was carried out

under positive ESI (electrospray ionization) using a Thermo scientific LTQ Orbitrap Discovery instrument.

3.2 Experimental Procedures

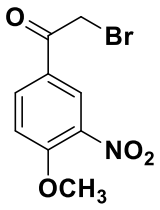

4'-Methoxy-3'-nitro-2-bromoacetophenone **2**[44, 45]

To a well-stirred solution of 4-methoxy-3-nitroacetophenone **1** (10.7 g, 54.5 mmol) in chloroform (50 mL) at room temperature, was added a solution of bromine (2.87 mL, 54.5 mmol) in chloroform (10 mL) dropwisely. The reaction mixture was stirred for 30 minutes. Water (50 mL) was added into the solution and the organic layer was separated and the aqueous layer was extracted with dichloromethane (3 X 45 mL). The combined organic layer was dried over Na_2SO_4 and concentrated under reduced pressure. The crude product was then recrystallized from hot ethanol to afford the desired bromoacetophenone derivative as yellow needle-shaped crystals **2** (14.4 g, 52.6 mmol, 95%), R_f = 0.48 (EtOAc/Hexanes: 30/70).

^{1}H NMR (600 MHz, Chloroform-*d*) δ 8.49 (d, *J* = 2.3 Hz, 1H), 8.22 (dd, *J* = 8.9, 2.3 Hz, 1H), 7.20 (d, *J* = 8.8 Hz, 1H), 4.40 (s, 2H), 4.07 (s, 3H).

^{13}C NMR (151 MHz, $CDCl_3$) δ 188.52, 156.77, 139.40, 134.89, 126.88, 126.23, 113.62, 57.08, 29.92.

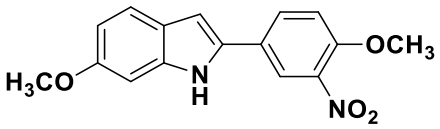

6-methoxy-2-(4-methoxy-3-nitrophenyl)indole **3**[44, 45]

To a solution of *m*-anisidine (4.72 mL, 42.1 mmol) in *N,N*-dimethylaniline (18mL) at 150 ^{o}C, a hot solution (60 ^{o}C) of bromide **2** (3.50 g, 12.8 mmol)in ethanol (15 mL) was added dropwisely. The reaction mixture was stirred at 160 – 170 ^{o}C for 12 hours. Water (20 mL) was added into the solution and organic layer was separated in a separation funnel. Aqueous layer was then extracted with EtOAc (3 X 30 mL). The combined organic phase was dried over Na_2SO_4 and concentrated under reduced pressure to afford a dark colored solid. This crude product was further purified by recrystallization from EtOAc to form the desired product as dark red powder **3** (.957 g, 3.22 mmol, 25%).

^{1}H NMR (600 MHz, Acetone-d6) δ 10.65 (s, 1H), 8.23 (d, *J* = 2.1 Hz, 1H), 8.08 (dd, *J* = 8.8, 2.2 Hz, 1H), 7.45 (t, *J* = 8.5 Hz, 2H), 6.95 (d, *J* = 2.0 Hz, 1H), 6.89 (d, *J* = 2.0 Hz, 1H), 6.73 (dd, *J* = 8.7, 2.1 Hz, 1H), 4.04 (s, 3H), 3.82 (s, 3H).

^{13}C NMR (151 MHz, $CDCl_3$) δ 157.81, 152.06, 141.38, 139.39, 135.29, 130.78, 126.82, 124.34, 121.84, 121.40, 115.58, 111.05, 100.47, 95.15, 57.20, 55.66.

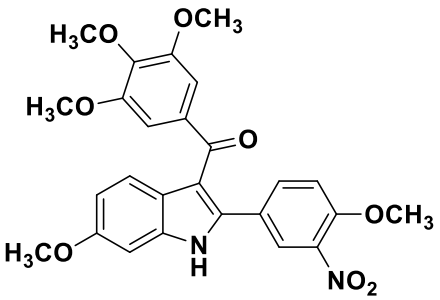

(6-methoxy-2-(4-methoxy-3-nitrophenyl)indol-3-yl)(3,4,5-trimethoxyphenyl)methanone **4**[44, 45]

To a solution of 6-methoxy-2-(4-methoxy-3-nitrophenyl)indole **3** (.559 g, 1.99 mmol) in *o*-dichlorobenzene (15 mL) at 150 ^{o}C, was added 3,4,5-trimethoxybenzoyl chloride (.782 g, 3.39 mmol) in portions. The reaction mixture was stirred at 160-170 ^{o}C for 12 hours. It was allowed to cool down to room temperature, filter and rinsed with a small amount of EtOAc. The residue was further purified by recrystallization from dichloromethane-hexanes to afford a greenish-yellow solid **4** (.485 g, 0.98 mmol, 50%).

^{1}H NMR (600 MHz, Methanol-d4) δ 7.92 (d, *J* = 8.8 Hz, 1H), 7.71 (d, *J* = 2.2 Hz, 1H), 7.63 (dd, *J* = 8.7, 2.3 Hz, 1H), 7.19 (d, *J* = 8.7 Hz, 1H), 7.00 (d, *J* = 2.2 Hz, 1H), 6.90 (dd, *J* = 8.8, 2.3 Hz, 1H), 6.81 (s, 2H), 3.92 (s, 3H), 3.87 (s, 3H), 3.69 (s, 6H), 3.69 (s, 3H).

^{13}C NMR (151 MHz, $CDCl_3$) δ 195.91, 156.17, 152.71, 152.23, 141.70, 139.95, 137.97, 135.82, 135.42, 130.20, 126.36, 125.05, 124.71, 122.28, 114.16, 109.72, 106.49, 106.21, 100.08, 61.03, 56.75, 56.35, 56.24.

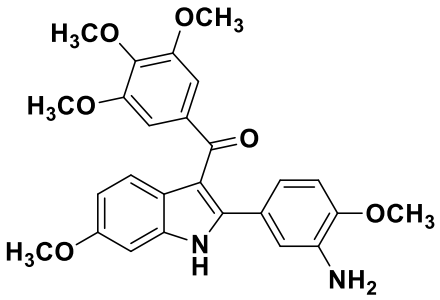

(2-(3-amino-4-methoxyphenyl)-6-methoxy-1H-indol-3-yl)(3,4,5-trimethoxyphenyl)methanone **5**

To a round-bottom flask with nitro compound **4** (246 mg, 0.497 mmol), 10% palladium on carbon (52.9 mg, 0.497 mmol) was added under nitrogen followed by MeOH (50 mL). Hydrogen was introduced through balloon. The reaction mixture was then stirred at room temperature for 2 hours examining periodically by TLC. It was filtered and the filtrate was concentrated under reduced pressure to achieve a yellow solid. The crude product was subjected to flash column chromatography using a pre-packed 10g silica gel column [solvent A, 50% EtOAc, 50% dichloromethane, solvent B, hexanes; gradient 20%A / 80%B (1CV), 20%A / 80%B → 90%A / 10%B (15 CV), 90%A / 10%B (6 CV); flow rate, 36 mL/min; monitored at 254 and 280 nm]. The final product amine **5** (186 mg, 0.402 mmol, 57%) was isolated as a yellow solid, R_f = 0.35, (EtOAc/Dichloromethane/hexane: 40/40/20).

^{1}H NMR (600 MHz, Chloroform-d) δ 8.46 (s, 1H), 7.90 (d, *J* = 9.3 Hz, 1H), 6.97 (s, 2H), 6.90 (dd, *J* = 4.7, 2.4 Hz, 2H), 6.69 (dd, *J* = 8.2, 2.1 Hz, 1H), 6.63 (d, *J* = 2.1 Hz, 1H), 6.59 (d, *J* = 8.2 Hz, 1H), 3.87 (s, 3H), 3.80 (s, 3H), 3.78 (s, 3H), 3.70 (s, 6H).

^{13}C NMR (151 MHz, $CDCl_3$) δ 191.98, 157.17, 152.44, 147.67, 143.06, 140.93, 136.19, 136.15, 134.94, 124.81, 123.11, 122.41, 119.22, 115.18, 112.63, 111.43, 109.93, 107.11, 94.49, 60.79, 56.00, 55.71, 55.51, 53.45.

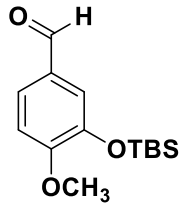

3-(tert-Butyldimethylsilyloxy)-4-methoxybenzaldehyde **7** [46]

To a solution of 3-hydroxy-4-methoxybenzaldehyde **6** (10.0 g, 65.8 mmol) dissolved in dichloromethane (200 mL) at 0 ^{o}C was added triethylamine (Et_3N) (10.1 mL, 72.3 mmol) followed by *N*,*N*-dimethylaminopyridine(DMAP) (0.804 g, 6.58 mmol). The reaction mixture was stirred for 10 min, and *tert*-butyldimethylsilyl chloride (TBSCl) (10.9 g, 72.3 mmol) was then added gradually. The solution was allowed to warm to room temperature over 12 h. Upon completion of the reaction, the reaction mixture was quenched with water (100 mL) and extracted with dichloromethane (3 X 50 mL). The extracted layers were combined, dried over Na_2SO_4, and concentrated under reduced pressure. The TBS benzaldehyde product **7** [17.3 g, 64.9 mmol, 99%, Rf = 0.47 (75:25 hexanes:EtOAc)] was isolated as a yellow oil and was taken to the next step without further purification.

^{1}H NMR ($CDCl_3$, 500 MHz): δ 9.80 (s, 1H, CHO), 7.45 (dd, *J* = 8.5 Hz, *J* = 2.0 Hz, 1H, ArH), 7.35 (d, *J* = 2.0 Hz, 1H, ArH), 6.93 (d, *J* = 8.5 Hz, 1H, ArH), 3.87 (s, 3H, OCH_3), 0.99 (s, 9H, $C(CH_3)_3$), 0.16 (s, 6H, $Si(CH_3)_2$).

^{13}C NMR ($CDCl_3$, 125 MHz): δ 190.2, 156.2, 145.2, 130.0, 126.0, 119.4, 110.9, 55.1, 25.3, 18.0, -5.0.

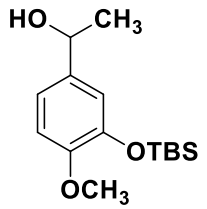

3-tert-Butyldimethylsilyloxy-1-(1'-hydroxyethyl)-4-methoxybenzene **8** [46]

Crude TBS benzaldehyde **7** (8.00 g, 30.1 mmol) dissolved in tetrahydrofuran (THF, 80 mL) at 0 ^{o}C was treated with CH_3Li (24.4 mL, 1.6 M, 39.1 mmol) dropwisely. The

solution was allowed to reach room temperature over 12 h. Upon completion of the reaction, the reaction mixture was slowly quenched with water (80 mL) and extracted with EtOAc (4 X 40 mL). The organic extract was dried over Na_2SO_4 and concentrated under reduced pressure, resulting in secondary alcohol **8** [8.22 g, 29.1 mmol, 97%, Rf = 0.31 (75:25 hexanes:EtOAc)] as a yellow oil, which was taken to the next step without further purification.

^{1}H NMR ($CDCl_3$, 500 MHz): δ 6.88 (m, 2H, ArH), 6.83 (d, *J* = 8.1 Hz, 1H, ArH), 4.81 (q, *J* = 6.3 Hz, 1H, CH), 3.79 (s, 3H, OCH_3), 1.82 (s, 1H, OH), 1.45 (d, *J* = 6.3 Hz, 3H, CH_3), 0.99 (s, 9H, $(CH_3)_3$), 0.15 (s, 6H, $Si(CH_3)_2$).

^{13}C NMR ($CDCl_3$, 125 MHz): δ 149.7, 144.5, 138.9, 118.4, 118.0, 111.7, 69.1, 55.1, 25.5, 24.9, 18.2, -4.8.

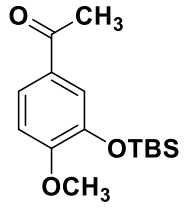

3-tert-Butyldimethylsilylox)-4-methoxyacetophenone **9** [46, 47]

To a solution of crude alcohol **8** (7.00 g, 25.0 mmol) and Celite® (6.00 g) in dichloromethane (75 mL) at 0 ^oC was added pyridinium chlorochromate (PCC, 5.91 g, 27.4 mmol) in small increments, allowing 10 min of stirring between each addition. The reaction mixture was allowed to warm to room temperature over 12 h. Upon completion of the reaction, the reaction mixture was filtered through a 50/50 plug of silica gel/Celite®, and the plug was rinsed well with dichloromethane. The filtrate was concentrated under reduced pressure providing the desired acetophenone

derivative **8** [6.35 g, 22.6 mmol, 89%, Rf = 0.59 (75:25 hexanes:EtOAc)] as a pale yellow solid.

^{1}H NMR ($CDCl_3$, 500 MHz): δ 7.57 (dd, *J* = 8.5 Hz, 2.0 Hz, 1H, ArH), 7.46 (d, *J* = 2.0 Hz, 1H, ArH), 6.86 (d, *J* = 8.5 Hz, 1H, ArH), 3.86 (s, 3H, OCH_3), 2.52 (s, 3H, CH_3), 1.00 (s, 9H, $C(CH_3)_3$), 0.16 (s, 6H, $Si(CH_3)_2$).

^{13}C NMR ($CDCl_3$, 125 MHz): δ 196.7, 155.3, 144.8, 130.5, 123.5, 120.4, 110.7, 55.4, 26.2, 25.6, 18.4, -4.7.

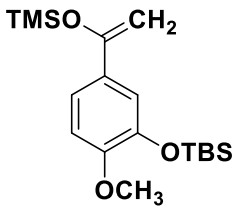

1-(3-tert-Butyldimethylsilyloxy-4-methoxyphenyl)-1-trimethylsilylethene **10** [47]

To a solution of diisopropylamine (2.88 mL, 20.4 mmol) in THF (100 mL) at 0 ^oC was added *n*-butyllithium (12.8 mL, 1.65 M, 20.4 mmol) dropwisely. The LDA solution was allowed to stir for 15 min, and then a solution of TBS-acetophenone **9** (3.82 g, 13.6 mmol) in THF (30 mL) was added dropwisely. The solution was stirred for 10 min, and trimethylsilyl chloride (TMSCl) (4.03 mL, 20.4 mmol) was added dropwisely. The reaction mixture was allowed to reach room temperature over 12 h. Upon completion of the reaction, the solution was diluted with $NaHCO_3$ (10%, 100 mL). The reaction mixture was extracted with Hexane (4 X 30 mL). Next the extract was dried over Na_2SO_4, and the organic phase was concentrated under reduced pressure to provide crude TMS-enol ether (4.41 g, 12.5 mmol, 92%) as a dark yellow oil, which was taken to the next step without purification.

^{1}H NMR ($CDCl_3$, 500 MHz): δ 7.18 (dd, *J* = 8.5 Hz, 2.5 Hz, 1H ArH), 7.12 (d, *J* = 2.5 Hz, 1H, ArH), 6.80 (d, *J* = 8.5 Hz, 1H, ArH), 4.78 (d, *J* = 1.5 Hz, 1H, CH_2), 4.34 (d, *J* = 1.5 Hz, 1H, CH_2), 3.81 (s, 3H, OCH_3), 1.03 (s, 9H, $C(CH_3)_3$), 0.27 (s, 9H, $Si(CH_3)_3$), 0.18 (s, 6H, $Si(CH_3)_2$).

^{13}C NMR ($CDCl_3$, 125 MHz): δ 155.3, 151.1, 144.4, 130.6, 118.8, 118.1, 111.2, 89.5, 55.4, 25.7, 18.4, 0.03, -4.7.

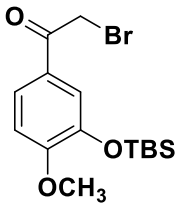

3'-(tert-Butyldimethylsilyloxy)-4'-methoxy-2-bromoacetophenone **11** [47]

To a solution of crude TMS-enol ether (4.41 g, 12.5 mmol) and anhydrous K_2CO_3 (.074 g, 0.538 mmol) in dichloromethane (40 mL) at 0 ^oC was added bromine (.362 mL, 7.5 mmol) dropwisely. The solution was allowed to stir for 30 min, diluted with sodium thiosulfate (10%) and extracted with dichloromethane (3 X 50 mL). The extract was dried over Na_2SO_4 and concentrated under reduced pressure. Purification by flash chromatography using a prepacked 100 g silica column [solvent A: EtOAc; solvent B: hexanes; gradient: 2%A / 98%B (4 CV), 2%A / 98%B → 20%A / 80%B (10 CV), 20%A / 80%B (1.2 CV); flow rate: 25 mL/min; monitored at 254 and 280 nm] afforded bromoacetophenone analogue **11** [1.60 g, 5.01 mmol, 40%, R_f = 0.37 (90:10 hexanes:EtOAc)] as a tan red solid.

^{1}H NMR ($CDCl_3$, 500 MHz): δ 7.61 (dd, *J* = 8.5 Hz, 2.5 Hz, 1H, ArH), 7.48 (d, *J* = 2.5 Hz, 1H, ArH), 6.88 (d, *J* = 8.5 Hz, 1H, ArH), 4.37 (s, 2H, CH_2), 3.88 (s, 3H, OCH_3), 1.00 (s, 9H, $C(CH_3)_3$), 0.17 (s, 6H, $Si(CH_3)_2$).

^{13}C NMR ($CDCl_3$, 125 MHz): δ 189.8, 156.1, 145.1, 127.1, 124.2, 121.0, 111.0, 55.5, 30.7, 25.6, 18.4, -4.6.

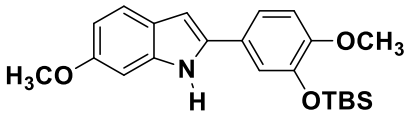

2-(3'-tert-Butyldimethylsilyloxy-4'-methoxyphenyl)-6-methoxyindole **12** [48]

To a solution of *m*-anisidine (3.02 mL, 27.0 mmol) dissolved in *N*,*N*-dimethylaniline (50 mL) at 170 ^oC was added dropwisely bromoacetophenone **11** (2.94 g, 8.18 mmol) in EtOAc (10 mL). The reaction mixture was stirred at 170 ^oC for 12 h. Upon completion of the reaction, the reaction mixture was cooled to room temperature and extracted with EtOAc (3 x 30 mL). The combined organic extract was dried over Na_2SO_4 and concentrated under reduced pressure. Purification by flash chromatography using a prepacked 100 g silica column [solvent A: EtOAc; solvent B: hexanes; gradient: 12%A / 88%B (4 CV), 12%A / 88%B → 100%A / 0%B (10 CV), 100%A / 0%B (2.6 CV); flow rate: 25 mL/min; monitored at 254 and 280 nm] resulted in the desired 2-phenylindole derivative **12** [1.87 g, 4.88 mmol, 60%, Rf = 0.48 (50:50 hexanes:EtOAc)] as light tan crystals.

^{1}H NMR ($CDCl_3$, 500 MHz): δ 8.11 (br s, 1H, NH), 7.47 (d, *J* = 8.5 Hz, 1H, ArH), 7.16 (dd, *J* = 8.5 Hz, 2.0 Hz 1H, ArH), 7.13 (d, *J* = 2.5 Hz, 1H, ArH), 6.90 (d, *J* = 8.5 Hz, 1H, ArH), 6.89 (d, *J* = 2.5 Hz, 1H, ArH), 6.79 (dd, *J* = 8.5 Hz, 2.5 Hz, 1H, ArH),

6.64 (dd, J = 2.0 Hz, 1.0 Hz 1H, ArH), 3.86 (s, 3H, OCH_3), 3.84 (s, 3H, OCH_3), 1.04 (s, 9H, $C(CH_3)_3$), 0.21 (s, 6H, $Si(CH_3)_2$).

^{13}C NMR ($CDCl_3$, 125 MHz): δ 156.3, 150.5, 145.4, 137.4, 136.9, 125.8, 123.7, 120.9, 118.2, 117.8, 112.4, 109.9, 98.6, 94.5, 55.6, 55.4, 25.7, 18.5, -4.6.

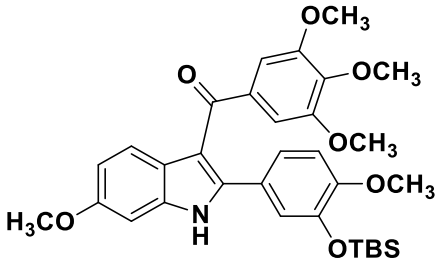

2-(3'-tert-Butyldimethylsiloxy-4'-methoxyphenyl)-3-(3",4",5"- trimethoxybenzoyl)-6-methoxyindole **13** [49]

To a solution of compound **12** (3.12 g, 8.14 mmol) in *o*-dichlorobenzene (30 mL) was added 3,4,5-trimethoxybenzoylchloride (2.82 g, 12.2 mmol). The reaction mixture was heated to reflux at 170 ^{o}C for 12 h. The *o*-dichlorobenzene was removed by simple distillation, and the resulting dark colored crude oil was subjected to flash chromatography using a prepacked 100 g silica column [solvent A: EtOAc; solvent B: hexanes; gradient: 10%A / 90%B (4 CV), 10%A / 90%B → 80%A / 20%B (10 CV), 80%A / 20%B (2.8 CV); flow rate: 40 mL/min; monitored at 254 and 280 nm] resulting in TBS-indole analogue **13** [1.60 g, 2.77 mmol, 34%, Rf = 0.38 (60:40 hexanes:EtOAc)] as a yellow powder.

^{1}H NMR (CDCl3, 500 MHz): δ 8.42 (br s, 1H, NH), 7.93 (d, J = 9.5 Hz, 1H, ArH), 6.99 (s, 2H, ArH) 6.94 (dd, J = 8.0 Hz, 2.0 Hz 1H, ArH), 6.91 (dd, J = 9.0 Hz, 2.0 Hz, 1H, ArH), 6.91 (d, J = 2.0 Hz, 1H, ArH), 6.77 (d, J = 2.0 Hz, 1H, ArH), 6.70 (d, J =

8.5 Hz, 1H, ArH), 3.87 (s, 3H, OCH_3), 3.79 (s, 3H, OCH_3), 3.74 (s, 3H, OCH_3), 3.69 (s, 6H, OCH_3), 0.94 (s, 9H, $C(CH_3)_3$), 0.04 (s, 6H, $Si(CH_3)_2$).

^{13}C NMR (CDCl3, 125 MHz): δ 191.9, 157.4, 152.6, 151.6, 145.2, 142.1, 141.3, 136.5, 134.6, 125.2, 123.4, 122.6, 122.3, 121.9, 112.9, 111.8, 111.7, 107.4, 94.6, 60.9, 56.1, 55.9, 55.5, 25.8, 18.5, -4.7.

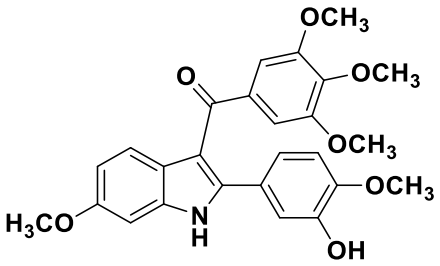

2-(3'-Hydroxy-4'-methoxyphenyl)-3-(3",4",5"-trimethoxybenzoyl)-6-methoxyindole **14** (**OXi8006**) [50]

To a well-stirred solution of compound **13** (1.33 g, 2.50 mmol) in THF (15 mL) at 0 ^{o}C was added tetrabutylammonium fluoride (TBAF·$3H_2O$, 1.18 mL, 3.75 mmol). The reaction mixture was stirred for 30 min while warming to room temperature. The reaction mixture was quenched with water (10mL) and extracted with EtOAc (3 x 10 mL). The combined organic extract was dried over Na_2SO_4 and concentrated under reduced pressure. Purification by flash column chromatography using a prepacked 50 g silica column [solvent A: EtOAc; solvent B: hexanes; gradient: 12%A / 88%B (1 CV), 12%A / 88%B → 100%A / 0%B (10 CV), 100%A / 0%B (5 CV); flow rate: 40 mL/min; monitored at 254 and 280 nm] afforded the desired phenolic indole **14** (**OXi8006**) [1.15 g, 2.48 mmol, 99%, Rf = 0.55 (10:90 MeOH:DCM)] as a yellow powder.

^{1}H NMR (CDCl3, 500 MHz): δ 8.30 (br s, 1H, NH), 7.93 (d, *J* = 9.5 Hz, 1H, ArH), 6.96 (s, 2H, ArH) 6.95 (d, *J* = 2.0 Hz, 1H, ArH), 6.93 (dd, *J* = 9.5 Hz, 2.5 Hz, 1H, ArH), 6.92 (d, *J* = 2.5 Hz, 1H, ArH), 6.78 (dd, *J* = 8.0 Hz, 2.0 Hz, 1H, ArH), 6.65 (d, *J* = 8.5 Hz, 1H, ArH), 5.55 (s, 1H, OH) 3.89 (s, 3H, OCH3), 3.84 (s, 3H, OCH3), 3.80 (s, 3H, OCH3), 3.71 (s, 6H, OCH3).

^{13}C NMR (CDCl3, 125 MHz): δ 192.7, 157.1, 152.5, 147.0, 145.3, 143.3, 141.0, 136.6, 135.0, 125.1, 123.0, 122.1, 121.5, 115.1, 112.6, 111.6, 110.3, 107.4, 94.8, 60.8, 56.0, 55.8, 55.6.

CHAPTER FOUR

Conclusions

The aim of this project was to not only synthesize new indole-based vascular disrupting agents, but also to further the field of targeting endothelial cells of blood vessels that supply tumor vasculature. As tumor cells are able to mutate, develop resistance against cell death, and even enhance their own proliferation and angiogenesis, current interventions will eventually prove to have diminished therapeutic efficacy in the future. Thus, targeting endothelial cells, which are unable to mutate and generate protection against therapeutic treatment, poses as a promising maneuver in the battle against cancer.

This project resulted in the successful synthesis of **OXi8006** as well as its nitro and amino analogues. Future studies will involve the use of **OXi8006** as a parent compound where various bioreductive triggers can be applied. This mechanism could potentially increase the efficacy and specificity of these vascular disrupting agents towards the hypoxic environment evident in tumor vasculature. In addition, the nitro and amino analogues of **OXi8006**, compound **4** and **5**, have been preliminarily evaluated for their ability to inhibit tubulin polymerization. In addition, compound **4** was also evaluated for its cytotoxicity against a variety of human cancer cell lines.

CHAPTER FIVE

References

1. Ahmad, A.S.; Ormiston-Smith, N.; Sasieni, P.D. Trends in the lifetime risk of developing cancer in Great Britain: Comparison of risk for those born from 1930 to 1960. *British Journal of Cancer*. **2015**. *112(5)*. 943-947.

2. Alexandrov, L.B.; Nik-Zainal, S.; Wedge, D.C.; Aparicio, S.A.J.R.; Behjati, S.; Biankin, A.V.; Bignell, G.R.; Bolli, N.; Borg, A.; Børresen-Dale, A.L. Signatures of mutational processes in human cancer. *Nature*. **2013**. *500(7463)*. 415-421.

3. Reeves, G.K.; Pirie, K.; Beral, V.; Green, J.; Spencer, E.; Bull, D.; Million Women Study Collaboration. Cancer incidence and mortality in relation to body mass index in the Million Women Study: Cohort study. *British Medical Journal*. **2007**. *335(7630)*. 1134.

4. Ruile, G.; Dianatliey, A.; Kriza, C.; Meier, F.; Leb, I.; Kalender, W.A.; Kolominsky-Rabas, P.L. Screening for breast cancer with Breast-CT in a ProHTA simulation. **2015**. *Journal of Comparative Effectiveness Research.*

5. Klotz, L. Active surveillance not only reduces morbidity, it saves lives. **2013**. *Cancer Network.*

6. Jordan, M.; Wilson, L. Microtubules As A Target for Anticancer Drugs. *Nature Reviews: Cancer*. **2004**. *4*, 253-265.

7. Davis, P.D.; Dougherty, G.J.; Blakey, D.C.; Galbraith, S.M.; Tozer, G.M.; Holder, A.L.; Naylor, M.A.; Nolan, J.; Stratford, M.R.L.; Chaplin, D.J.; Hill, S.A. ZD6126: a novel vascular-targeting agent that causes selective destruction of tumor vasculature. *Cancer Research.* **2002**. *62*, 7247–7253.

8. Monk, K.A.; Siles, R.; Hadimani, M.B.; Mugabe, B.E.; Ackley, J. Freeland; Studerus, S.W.; Edvardsen, K.; Trawick, M.; Garner, C.M.; Rhodes, M.R.; Pettit, G.R.; Pinney, K.G. Design, synthesis, and biological evaluation of combretastatin nitrogen-containing derivatives as inhibitors of tubulin assembly and vascular disrupting agents. *Bioorganic & Medicinal Chemistry*. **2006**. *14*. 3231-3244.

9. Flynn, B.L.; Gill, G.S.; Grobelny, D.W.; Chaplin, J.H; Paul, D.; Leske, A.F.; Lavranos, T.C.; Chalmers, D.K.; Charman, S.A.; Kostewicz, E.; Shackleford, D.M.; Morizzi, J.; Hamel, E.; Jung, M.K.; Kremmidiotis, G. Discovery of 7-

Hydroxy-6-methoxy-2-methyl-3-(3,4,5-trimethoxybenzoyl)benzo[b]benzofuran (BNC105), a Tubulin Polymerization Inhibitor with Potent Antiproliferative and Tumor Vascular Disrupting Properties. *J. Med. Chem*. **2011**. *54*. 6014-6027.

10. Liou, J.; Chang, Y.; Kuo, F.; Chang, C.; Tseng, H.; Wang, C.; Y.; Chang, J.; Lee, S.; Hsich, H. Concise Synthesis and Structure-Activity Relationships of Combretastatin A-4 Analogues, 1-Aroylindoles and 3-Aroylindoles, as Novel Classes of Potent Antitubulin Agents. *Journal of Medicinal Chemistry*. **2004**. *47*, 4247-4257.

11. Silvestri, R. "New Prospects for Vinblastine Analogues as Anticancer Agents." *Journal of Medicinal Chemistry.* **2013**. *56,* 625-627.

12. Miller, M.L.; Ohima, I. Chemistry and Chemical Biology of Taxane Anticancer Agents. *The Chemical Record*. **2001**. *1*. 195-211.

13. Desai, A.; Mitchison, T.J. Microtubule polymerization dynamics. *Annual Review of Cell and Developmental Biology*. **1997**. *13*. 83-117.

14. Mason, R.P.; Zhao, D.; Liu, L.; Trawick, M.; Pinney, K.G. A Perspective on Vascular Disrupting Agents that Interact with Tubulin: Preclinical Tumor Imaging and Biological Assessment. *Integrative. Biology*. **2011**, *3*, 375−387.

15. Strecker, T.E.; Odutola, S.O.; Lopez, R.; Cooper, M.S.; Tidmore, J.K.; Charlton-Sevcik, A.K.; Li, L.; MacDonough, M.T.; Hadimani, M.B.; Ghatak, A.; Liu, L.; Chaplin, D.J.; Mason, R.P.; Pinney, K.G.; Trawick, M.L. The vascular disrupting activity of OXi8006 in endothelial cells and its phosphate prodrug OXi8007 in breat tumor xenografts. *Cancer Letters*. **2015**. *369*. 229-241.

16. Tozer, G.M.; Kanthou, C.; Baguley, B.C. Disrupting tumour blood vessels. *Nature Reviews Cancer*. **2005**. *5(6)*. 423-435.

17. Lippert III, J.W. Vascular Disrupting Agents. *Science Direct*. **2006**. *15*, 605-615.

18. Siemann, D.W.; Bibby, M.C.; Dark, G.G.; Dicker, A.P.; Eskens, F.A.L.M.; Horsman, M.R.; Marmé, D.; LoRusso, P.M. Differentiation and Definition of Vascular-Targeted Therapies. *Clinical Cancer Research*. **2005**. *11*, 416.

19. Giannakakou, P.; Sackett, D.; Fojo, T. Tubulin/microtubules: Still a promising target for new chemotherapeutic agents. *Journal of the Natural Cancer Institute*. **2000.** *92.* 182-183**.**

20. Lu, Y.; Chen, J.; Xiao, M.; Li, W.; Miller, D.D. An overview of tubulin inhibitors that interact with the Colchicine binding site. *Pharmaceutical Research*. **2012**. *29(11)*. 2943-2971.

21. Pettit, G.R.; Cragg, G.M.; Herald, D.L.; Schmidt, J.M.; Lohavanijaya, P. Isolation and structure of combretastin. *Canadian Journal of Chemistry*. **1982**. *60*. 1374-1376.

22. Zawilska, J.B.; Wojcieszak, J.; Olejniczak, A.B. Prodrugs: A challenge for the drug development. *Pharmacological Reports*. **2013**. *65*. 1-14.

23. MacDonough, M.T.; Strecker, T.E.; Hamel, E.; Hall, J.H.; Chaplin, D.J.; Trawick, M.; Pinney, K.G. Synthesis and biological evaluation of indole-based, anti-cancer agents, inspired by the vascular disrupting agent 2-(3'-hydroxy-4'-methoxyphenyl)-3-(3",4",5"-trimethoxybenzoyl)-6-methoxyindole (OXi8006). **2013**. *Bioorganic & Medicinal Chemistry*. *21(21)*. 6831-6843.

24. Leggans, E.K.; Duncan, K.K.; Barker, T.J.; Schleicher, K.D.; Boger, D.L. A Remarkable Series of Vinblastine Analogues Displaying Enhanced Activity and an Unprecedented Tubulin Binding Steric Tolerance: C20' Urea Derivatives. *Journal of Medicinal Chemistry.* **2013**. *56*, 628-639.

25. Guénard, D.; Guêritte-Voegelein, F.; Potier, P. Taxol and Taxotere: Discovery, Chemistry, and Structure-Activity Relationships. *Accounts of Chemical Research*. **1993**. *26*. 160-167.

26. Ojima, I.; Slater, J.C.; Michaud, E.; Kuduk, S.D.; Bounaud, P.Y.; Vrignaud, P.; Bissery, M.C.; Veith, J.M.; Pera, P.; Bernacki, R.J. Syntheses and structure-activity relationships of the second-generation antitumor taxoids: Exceptional activity against drug-resistance cancer cells. *Journal of Medicinal Chemistry*. **1996**. *39(20)*. 3889-3896.

27. Kirschner, L.S.; Greenberger, L.M.; Hsu, S.I.-H.; Yang, C.-P. H.; Cohen, D.; Piekarz, R.L.; Castillo, G.; Han, E.K.-H. H.; Yu, L.; Horwitz, S.B. Biochemical and genetic characterization of the multidrug resistance phenotype in murine macrophage-like J774.2 cells. *Biochemistry Pharmacology*. **1992**. *43*. 77.

28. Ferlini, C.; Distefano, M.; Pignatelli, F.; Lin, S.; Riva, A.; Bombardelli, E.; Mancuso, S.; Ojima, I.; Scambia, G. Antitumor activity of novel taxanes that act at the same time as cytotoxic agents and P-glycoprotein inhibitors. *British Journal of Cancer*. **2000**. *83(12)*. 1762-1768.

29. Hadimani, M.B.; MacDonough, M.T.; Ghatak, A.; Strecker, T.E.; Lopez, R.; Sriram, M.; Nguyen, B.L.; Hall, J.J.; Kessler, R.J.; Shirali, A.R.; Liu, L.; Garner, C.M.; Pettit, G.R.; Hamel, E.; Chaplin, D.J.; Mason, R.P; Trawick, M.; Pinney, K.G. Synthesis of a 2-Aryl-3-aroyl Indole Salt (OXi8007) Resembling Combretastatin A-4 with Application as a Vascular Disrupting Agent. *Journal of Natural Products*. **2013**. *76,* 1668-1678.

30. MacDonough, M.T.; Shi, Z.; Pinney, K.G. Mechanistic considerations in the synthesis of 2-aryl-indole analogues under Bischler-Mohlau conditions. *Tetrahedron Letters*. **2015**. *56*. 3624-3629.

31. Pinney, K.G.; Bounds, A.D.; Dingeman, K.M.; Mocharla, V.P.; Pettit, G.R.; Bai, R.; Hamel, E.A. A new anti-Tubulin agent containing the benzo[b]thiophenes ring system. *Bioorganic & Medicinal Chemistry Letters*. **1999**. *9*. 1081-1086.

32. Pinney, K.G.; Pettit, G.R.; Mocharla, V.P.; Pilar, M.; Shirali, A. WO US 6350777 BS 20020226

33. Hadimani, M.B.; Kessler, R.J.; Kautz, J.A.; Ghatak, A.; Shirali, A.R.; O'dell, H.; Garner, C.M.; Pinney, K.G. 2-(3-tert-Butyldimethylsiloxy-4-methoxyphenyl)-6-methoxy-3-(3,4,5-Trimethoxybenzoyl)indole. *Acta Crystallographica*. **2002.** *C58*. 330-332.

34. Pinney, K. G.; Wang, F.; Del Pilar Mejia, M. PCT Int. Appl. 2001, WO 2001019794 A2 20010322.

35. Nancy, T.; Dupeyre, G.; Chabot, G.G.; Seguin, J.; Tillequin, F.; Scherman, D.; Michel, S.; Cachet, X. Synthesis and Biological Evaluation of New Disubstituted Analogues of 6-Methoxy-3-(3′,4′,5′-Trimethoxybenzoyl)-1H-Indole (BPR0L075), as Potential Antivascular Agents. *Bioorganic & Medicinal Chemistry*. **2008**. *16,* 7494–7503.

36. Horsman, M.R.; Siemann, D.W. Pathophysiologic Effects of Vascular-Targeting Agents and the Implications for Combination with Conventional Therapies. *Cancer Research*. **2006**. *66*, 11520–11539.

37. Guise, Christopher P.; Mowday, Alexandra M.; Ashoorzadeh, Amir; Yuan, Ran; Lin, Wan-Hua; Wu, Dong-Hai; Smaill, Jeff B.; Patterson, Adam V.; Ding, Ke. Bioreductive prodrugs as cancer therapeutics: targeting tumor hypoxia. *Chinese Journal of Cancer*. **2014**. *33.2*, 80-86.

38. Wilson, W.R.; Hay, M.P. Targeting hypoxia in cancer therapy. *Nature Reviews*. **2011.** *11*. 393-410.

39. Nordsmark, M.; Overgaard, M.; Overgaard, J. Pretreatment oxygenation predicts radiation response in advanced squamous cell carcinoma of the head and neck. *Radiotherapy & Oncology*. **1996**. *41,* 31-39.

40. Strecker, T. E.; Odutola, S. O.; Sevcik, A. K.; Tanpure, R. P.; George, C. S.; Chaplin, D. J.; Trawick, M. L.; Pinney, K. G. 68th Southwest Regional Meeting of the American Chemical Society, Waco TX, **2013**

41. Sun, J.D.; Lie, Q.; Wang, J.; Ahluwalia, D.; Ferraro, D.; Wang, Y.; Duan, J.; Ammons, W.S.; Curd, J.G.; Matteucci, M.D.; Hart, C.P. Selective Tumor

Hypoxia Targeting by Hypoxia-Activated Prodrug TH-302 Inhibits Tumor Growth in Preclinical Models of Cancer. *Clinical Cancer Research*. **2012**. *18(3)*. 758-770.

42. Benito, J.; Shi, Y.; Szymanska, B.; Carol, H.; Boehm, I.; Lu, H.; Konoplex, S.; Fang, W.; Zweidler-McKay, P.A.; Campana, D.; Borthakur, G.; Bueso-Ramos, C.; Shpall, E.; Thomas, D.A.; Jordan, C.T.; Kantarjain, H.; Wilson, W.R.; Lock, R.; Andreeff, M.; Konopleva, M. Pronounced Hypoxia in Models of Murine and Human Leukemia: High Efficacy of Hypoxia-Activated Prodrug PR-104. *PLoS One*. **2011**. *6(8)*.

43. Guise, C.P.; Abbattista, M.R.; Singleton, R.S.; Holford, S.D.; Connolly, J.; Dachs, G.U.; Fox, S.B.; Pollock, R.; Harvey, J.; Guilford, P.; Doñate, F.; Wilson, W.R.; Patterson, A.V. The bioreductive prodrug PR-104 is activated under aerobic conditions by human aldo-keto reductase 1C3. *Cancer Research*. **2010**. *70(4)*. 1573-1584.

44. Hadimani, M.B. Studies toward the discovery of new classes of privileged molecules as colchicine-site binding ligands for tubulin: Structure-based design, synthesis, and bioactivity of small ligands targeted at tumor vasculature. Doctoral dissertation, Baylor University, **2004**.

45. Pinney, K.G.; Wang, F.; Hadimani, M.; Del Pilar Mejia, M. From PCT Int. Appl. **2004**, WO 20070082872 A1 20070412.

46. Tanpure, R. P.; Harkrider, A. R.; Strecker, T. E.; Hamel, E.; Trawick, M. L.; Pinney, K. G. Bioorg. Med. Chem. *17*: 6993-7001, **2009**.

47. Pinney, K. G.; Mocharla, V. P.; Chen, Z.; Garner, C. M.; Ghatak, A.; Hadimani, M.; Kessler, J.; Dorsey, J. M. PCT Int. Appl. WO 2001068654 A2 20010920, 2001.

48. Pinney, K.; Wang, F.; Hadimani, M.; Del Pilar Mejia, M.; From PCT Int. Appl. **2004**, WO 2004099139 A1 20041118.

49. Hadimani, M. B.; Kessler, R. J.; Kautz, J. A.; Ghatak, A.; Shirali, A. R.; O'dell, H.; Garner, C. M.; Pinney, K. G. *Acta. Cryst.* **2002**, *C58*, 330-332.

50. Pinney, K. G.; Wang, F.; Del Pilar Mejia, M. From PCT Int. Appl. **2001**, WO 2001019794 A2 20010322.

CHAPTER SIX

Supplementary Data

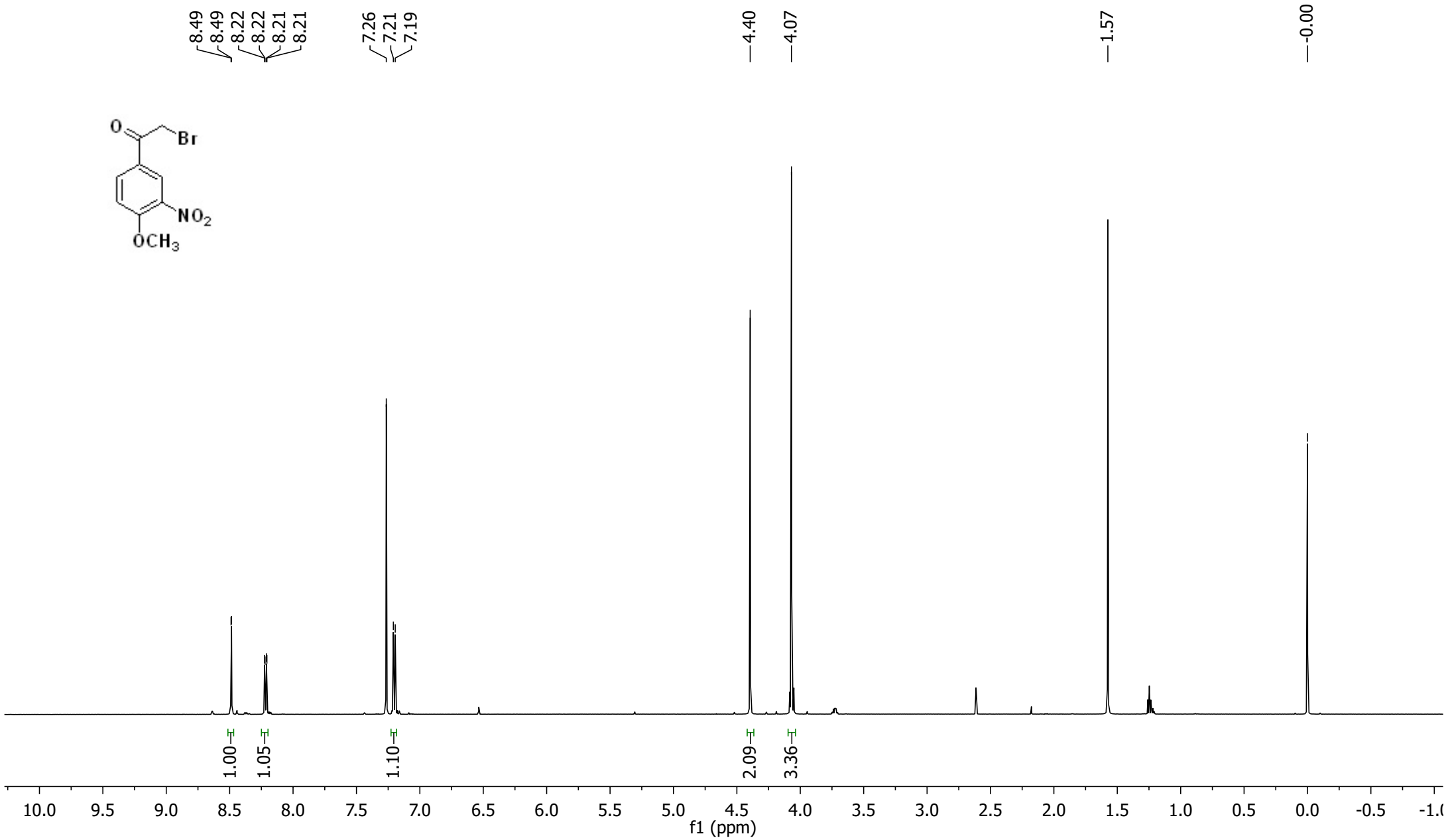

1H NMR (600 MHz) for Compound **2**

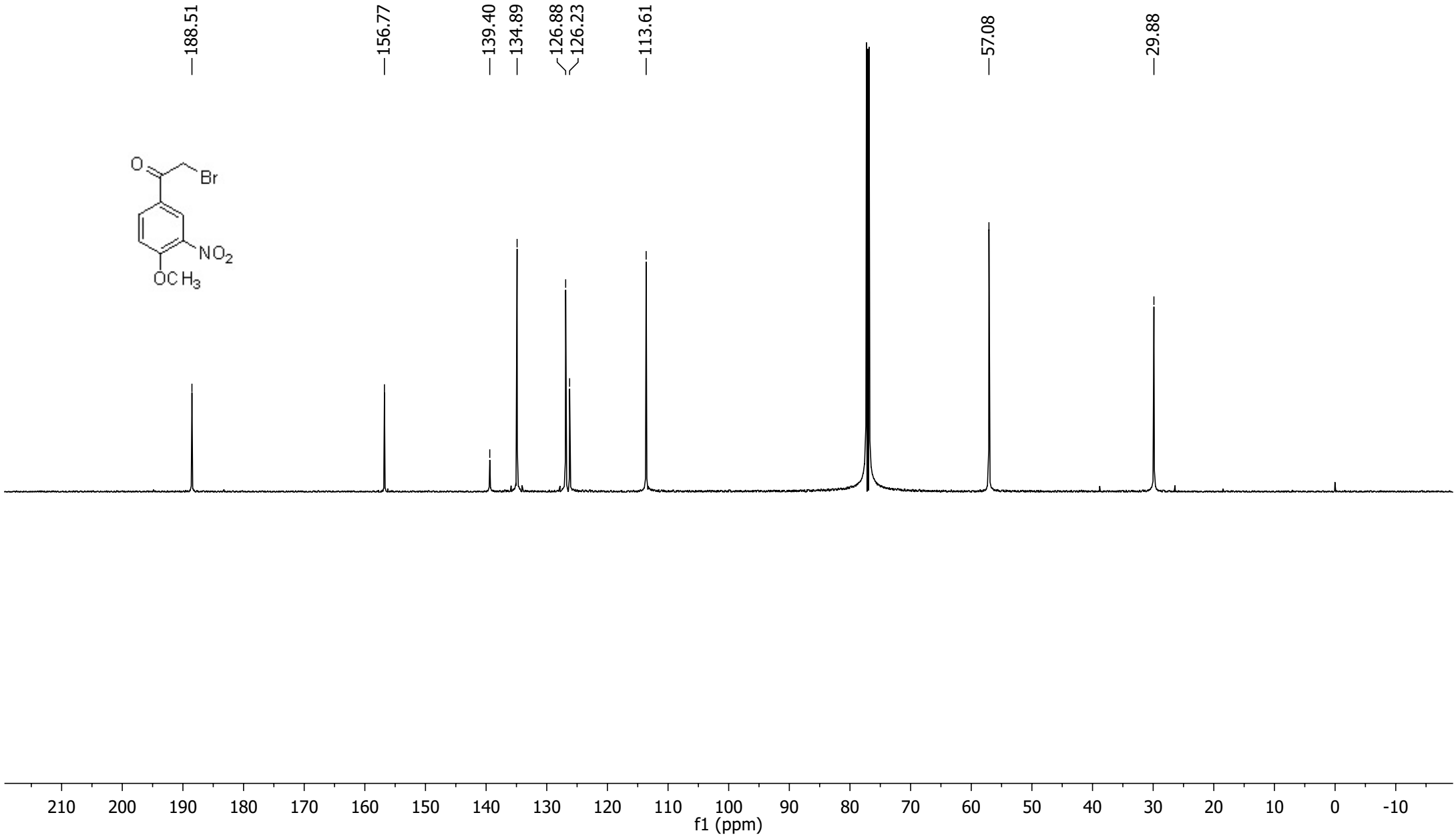

13C NMR (125 MHz) for Compound **2**

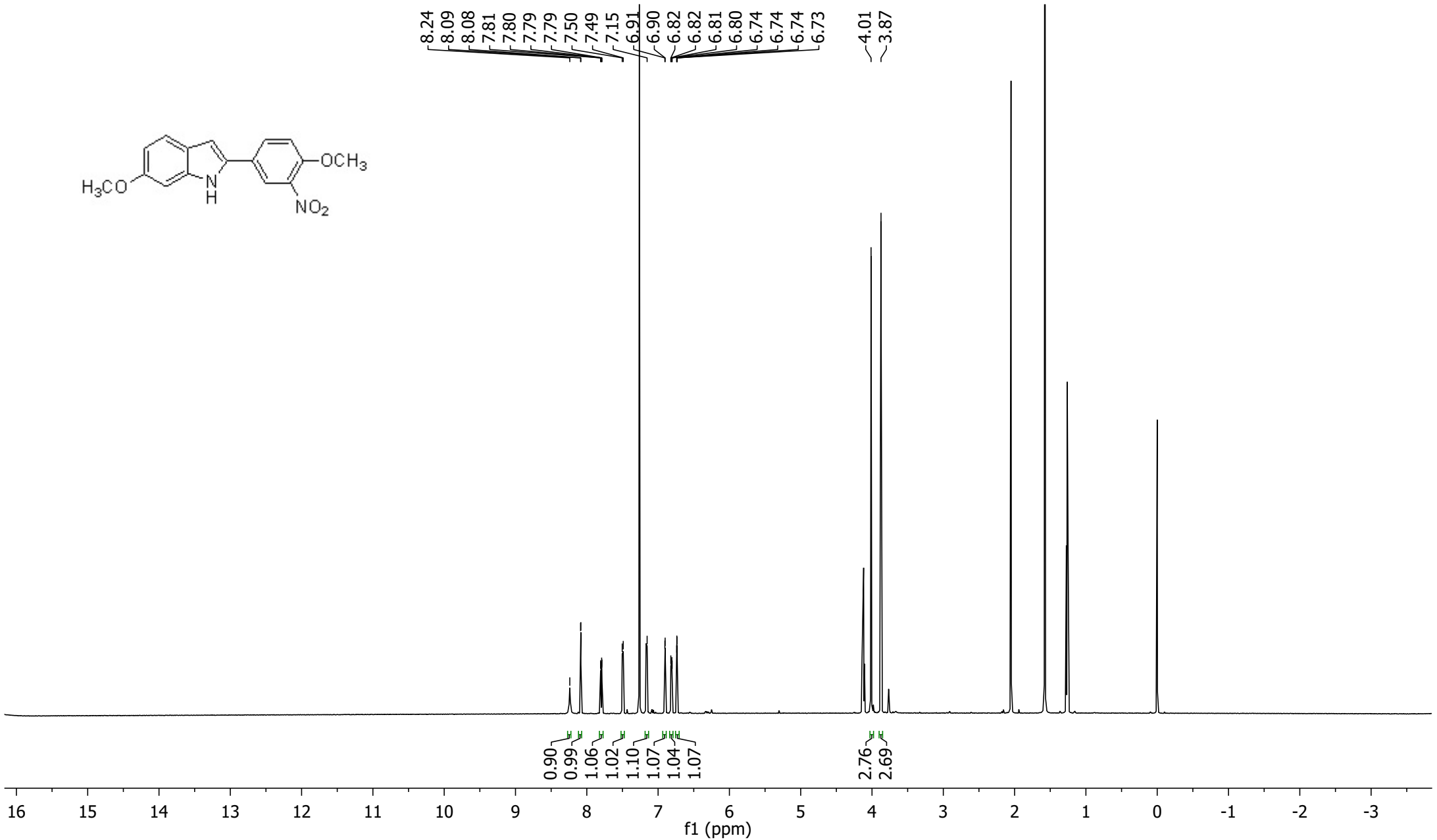

1H NMR (600 MHz) for Compound 3

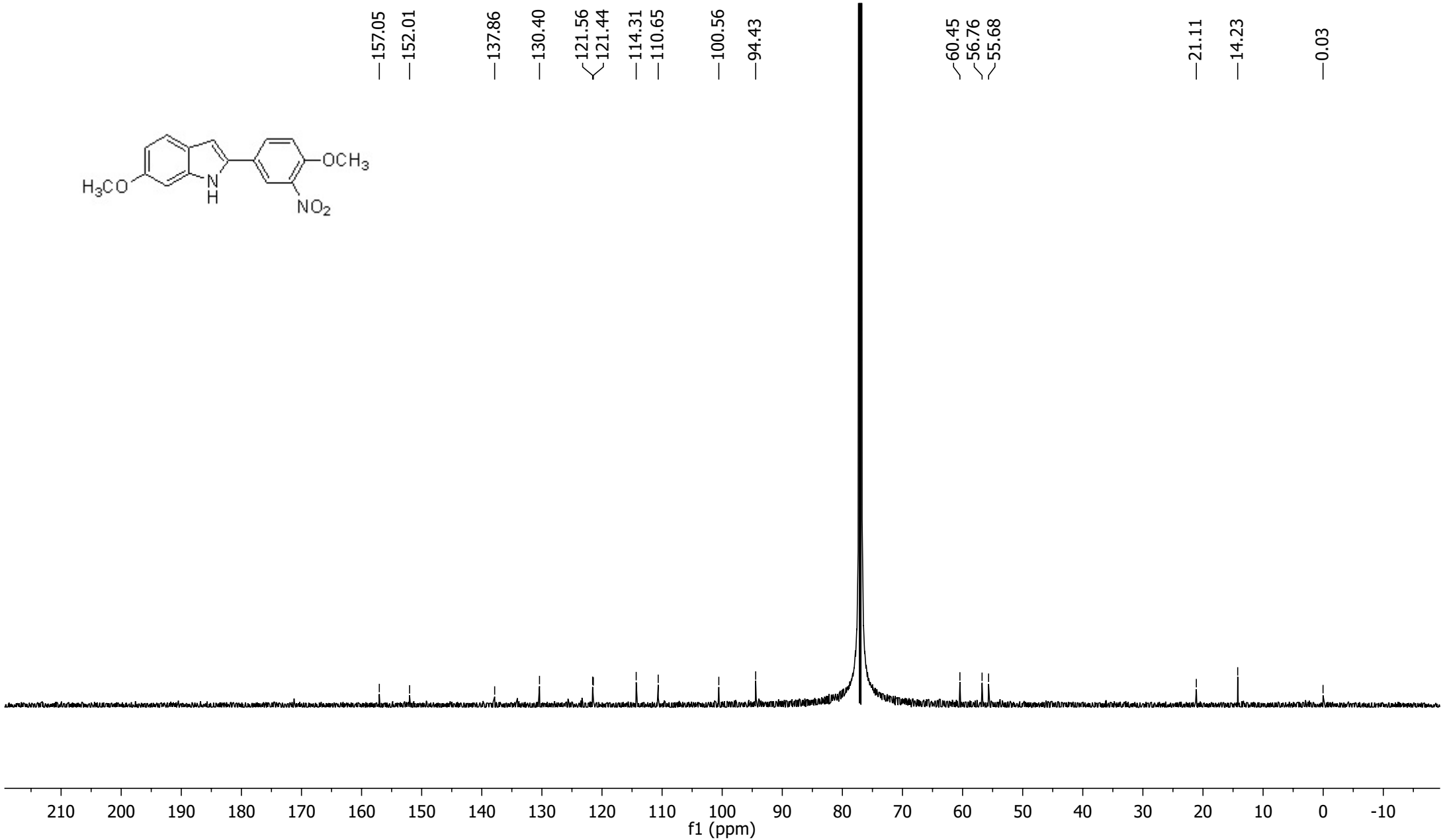

13C NMR (125 MHz) for Compound **3**

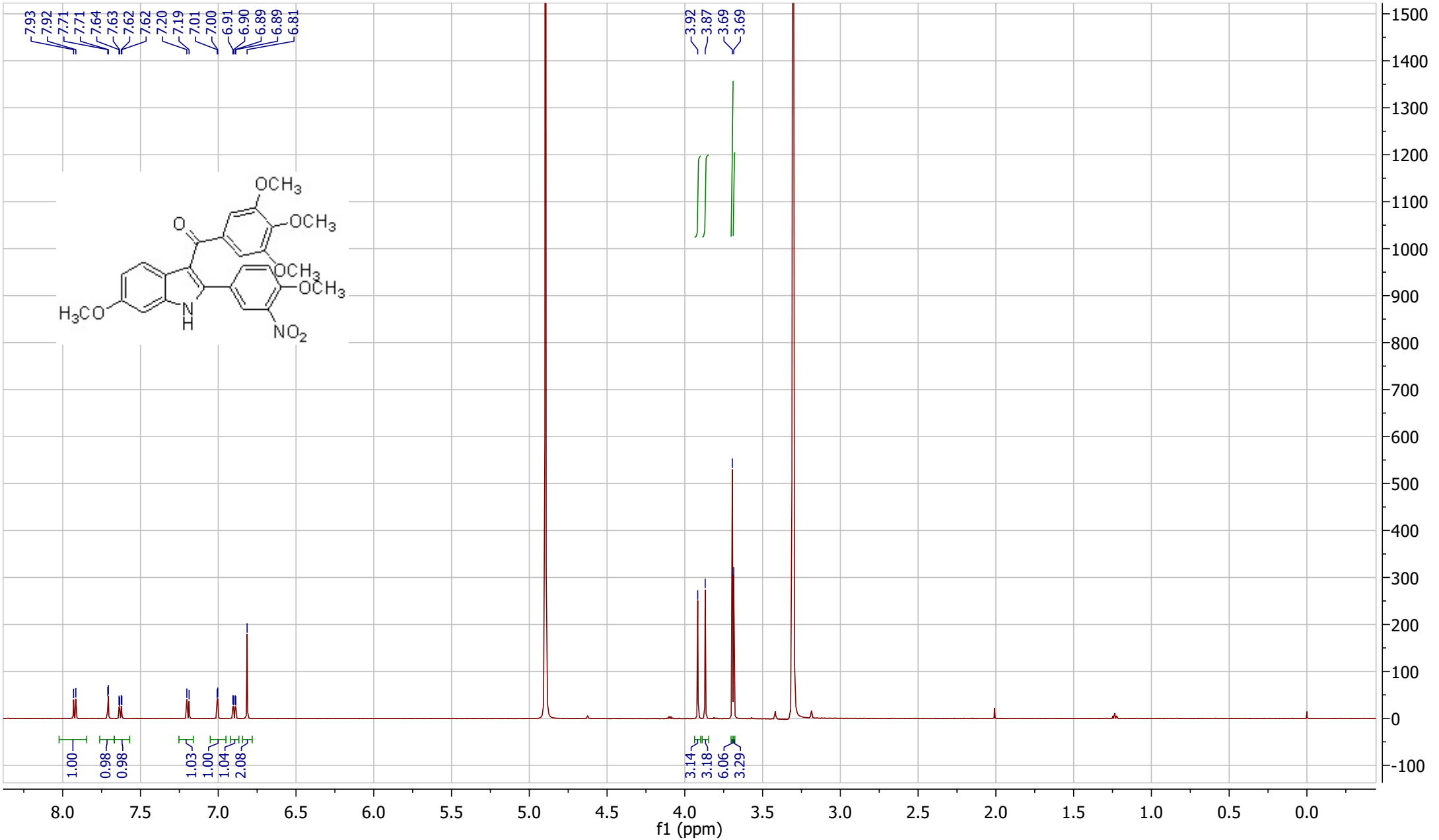

1H NMR (600 MHz) for Compound **4**

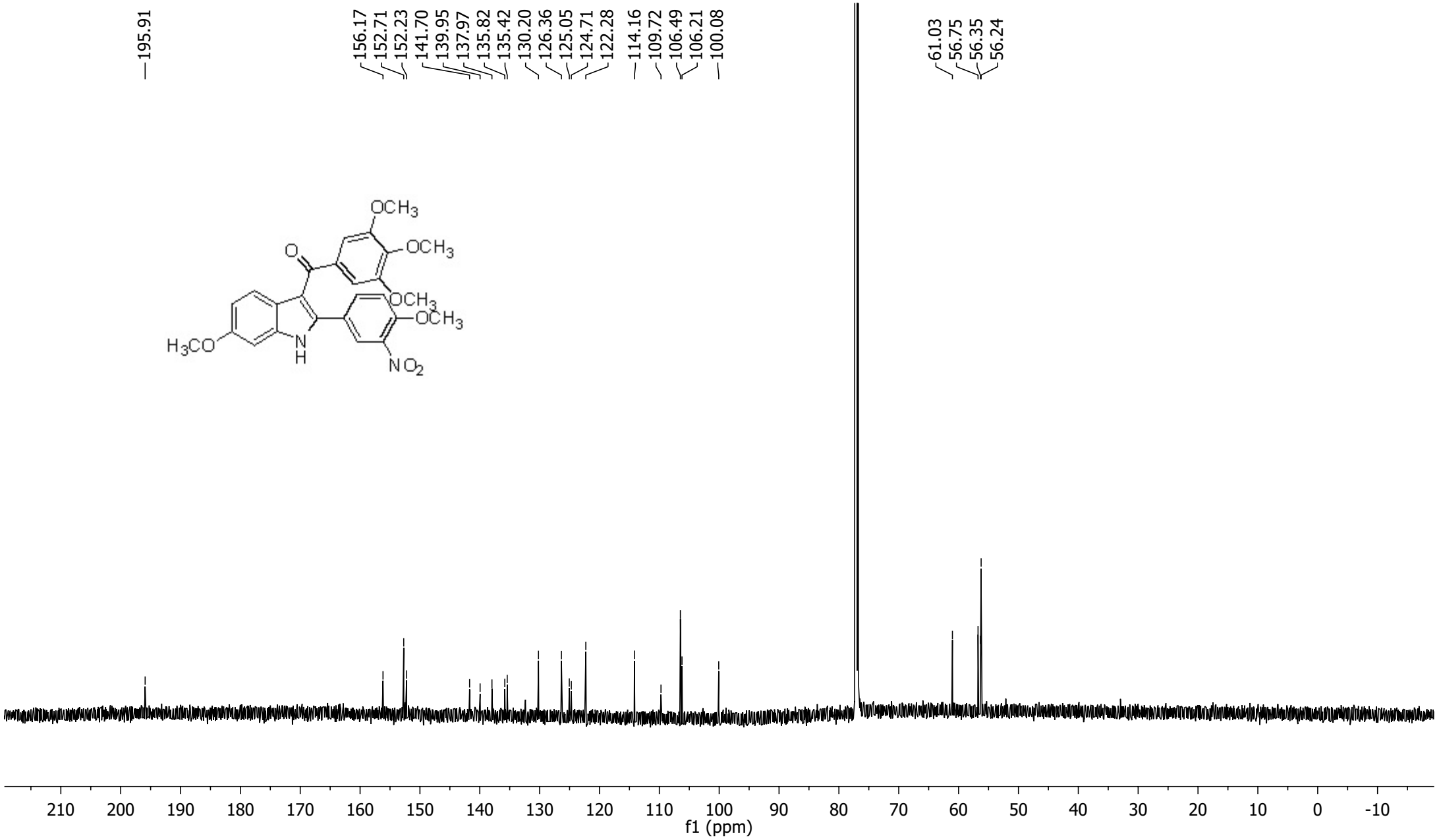

13C NMR (125 MHz) for Compound **4**

HRMS for Compound 4

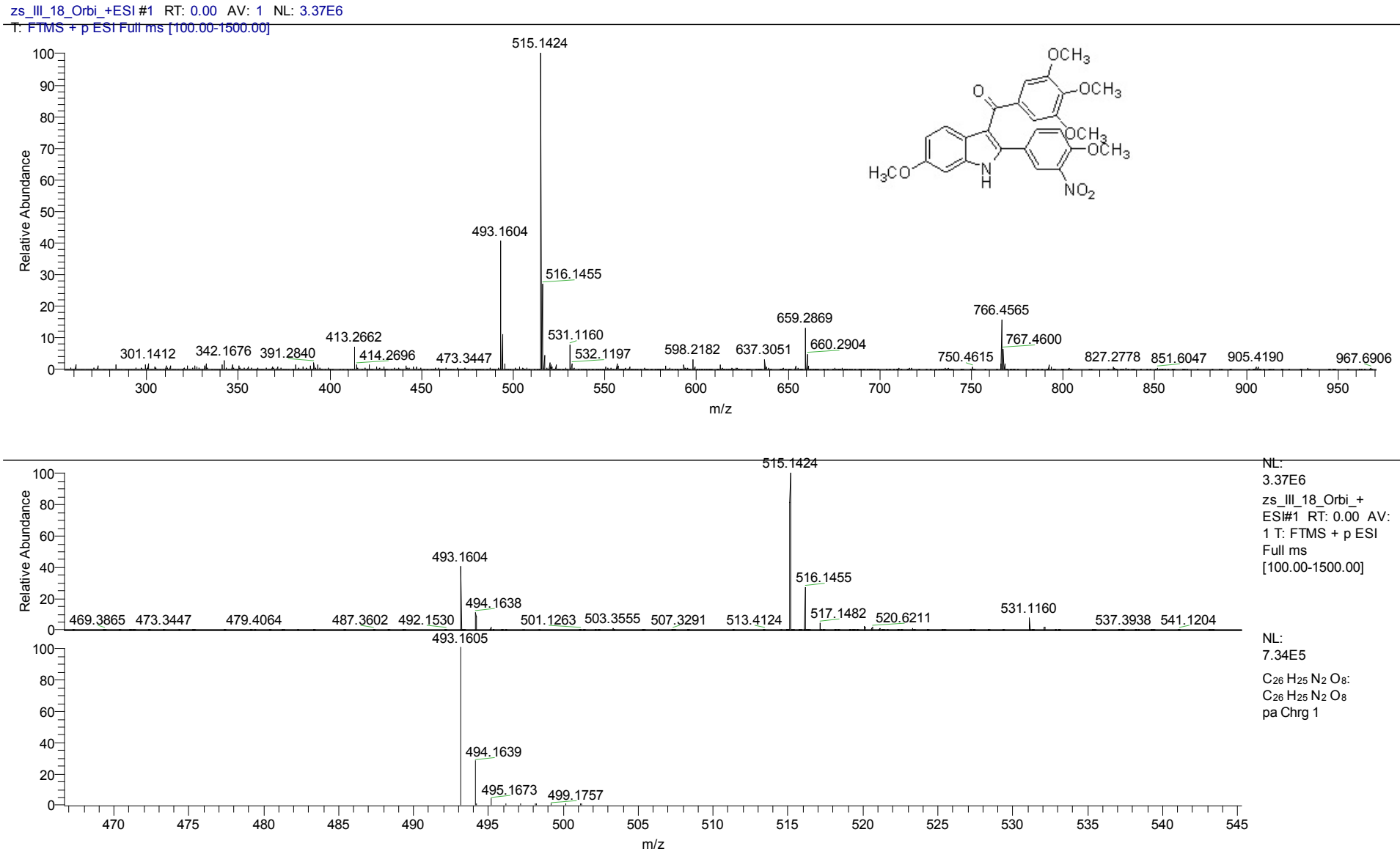

HPLC Trace for Compound 4

```
==========================================================================
Acq. Operator   : zhe
Acq. Instrument : Instrument 1                    Location :   -
Injection Date  : 7/25/2015 4:18:01 PM
Acq. Method     : C:\CHEM32\1\METHODS\GRAD 2 50-90 ACN.M
Last changed    : 7/25/2015 4:11:41 PM by zhe
Analysis Method : C:\CHEM32\1\DATA\ZHE\ZS_III_18000071.D\DA.M (GRAD 2 50-90 ACN.M)
Last changed    : 7/27/2015 6:04:46 PM by zhe
Sample Info     : zs_III_18
                  20150724
                  GRAD 2 50-90-ACN
```

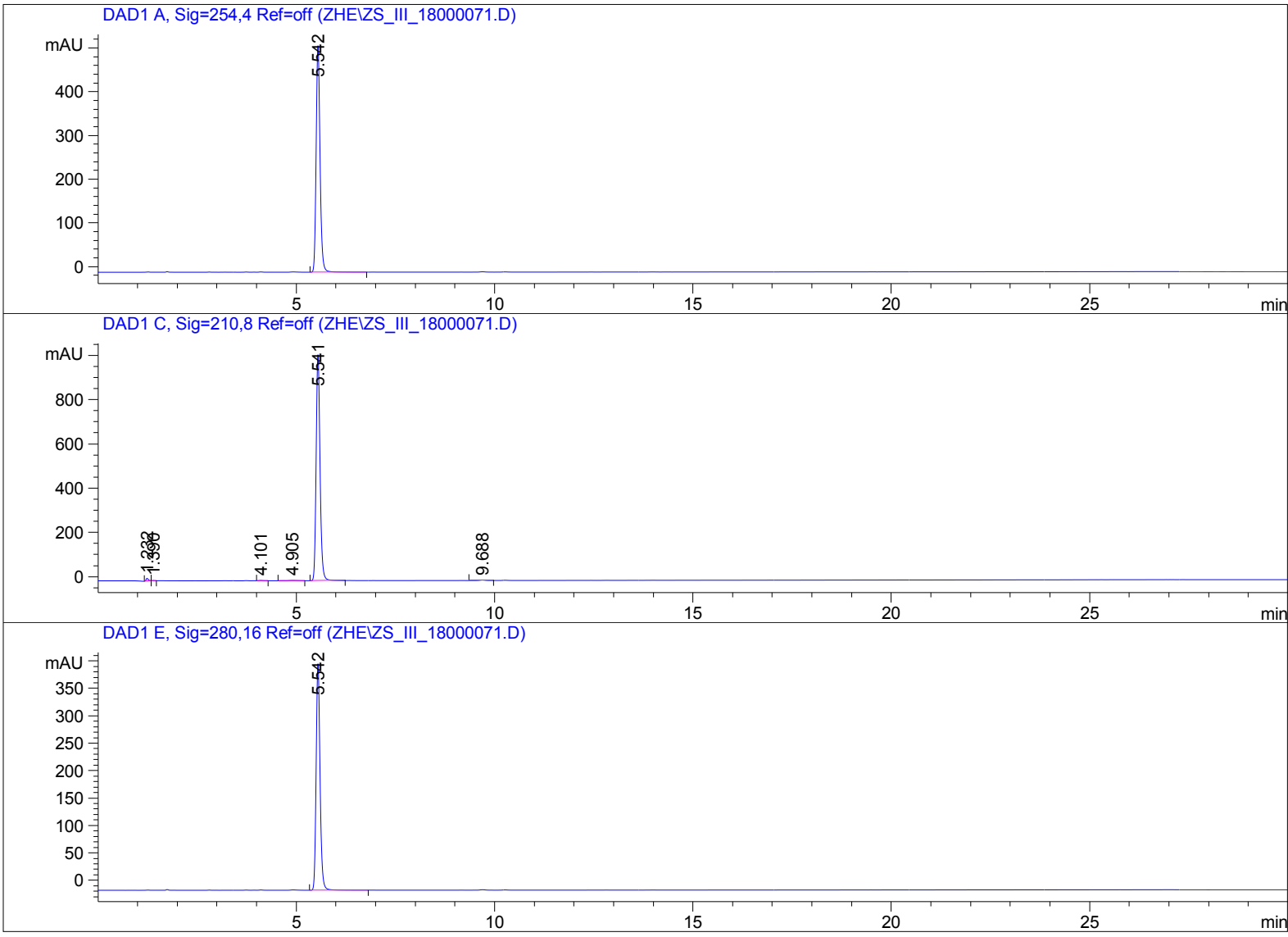

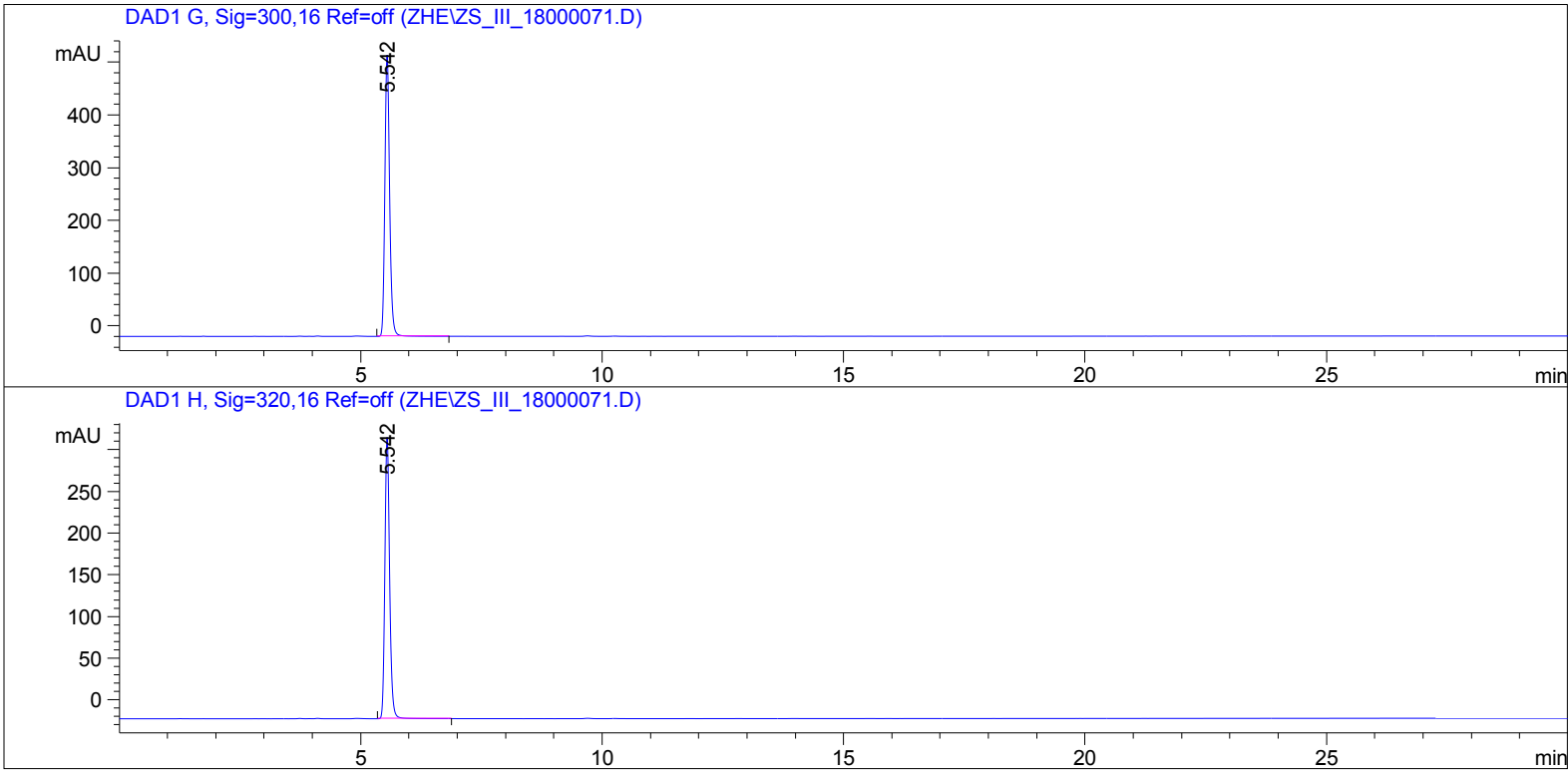

==========

Area Percent Report

==========

Sorted By : Signal
Multiplier : 1.0000
Dilution : 1.0000
Use Multiplier & Dilution Factor with ISTDs

Signal 1: DAD1 A, Sig=254,4 Ref=off

Peak #	RetTime [min]	Type	Width [min]	Area [mAU*s]	Height [mAU]	Area %
1	5.542	BB	0.1055	3531.82935	518.12195	100.0000
Totals :				3531.82935	518.12195	

Signal 2: DAD1 C, Sig=210,8 Ref=off

Peak #	RetTime [min]	Type	Width [min]	Area [mAU*s]	Height [mAU]	Area %
1	1.232	BV	0.0684	53.55264	12.40019	0.7589
2	1.390	VB	0.0749	7.52131	1.44099	0.1066
3	4.101	BB	0.0884	7.05204	1.23912	0.0999
4	4.905	BB	0.1966	15.27252	1.19934	0.2164

Peak #	RetTime [min]	Type	Width [min]	Area [mAU*s]	Height [mAU]	Area %
5	5.541	BB	0.1055	6955.45752	1020.71185	98.5669
6	9.688	BB	0.1417	17.72804	1.92016	0.2512
Totals :				7056.58407	1038.91165	

Signal 3: DAD1 E, Sig=280,16 Ref=off

Peak #	RetTime [min]	Type	Width [min]	Area [mAU*s]	Height [mAU]	Area %
1	5.542	BB	0.1056	2816.50708	413.00449	100.0000
Totals :				2816.50708	413.00449	

Signal 4: DAD1 G, Sig=300,16 Ref=off

Peak #	RetTime [min]	Type	Width [min]	Area [mAU*s]	Height [mAU]	Area %
1	5.542	BB	0.1056	3639.63867	533.39392	100.0000
Totals :				3639.63867	533.39392	

Signal 5: DAD1 H, Sig=320,16 Ref=off

Peak #	RetTime [min]	Type	Width [min]	Area [mAU*s]	Height [mAU]	Area %
1	5.542	BB	0.1056	2303.17480	337.51797	100.0000
Totals :				2303.17480	337.51797	

*** End of Report ***

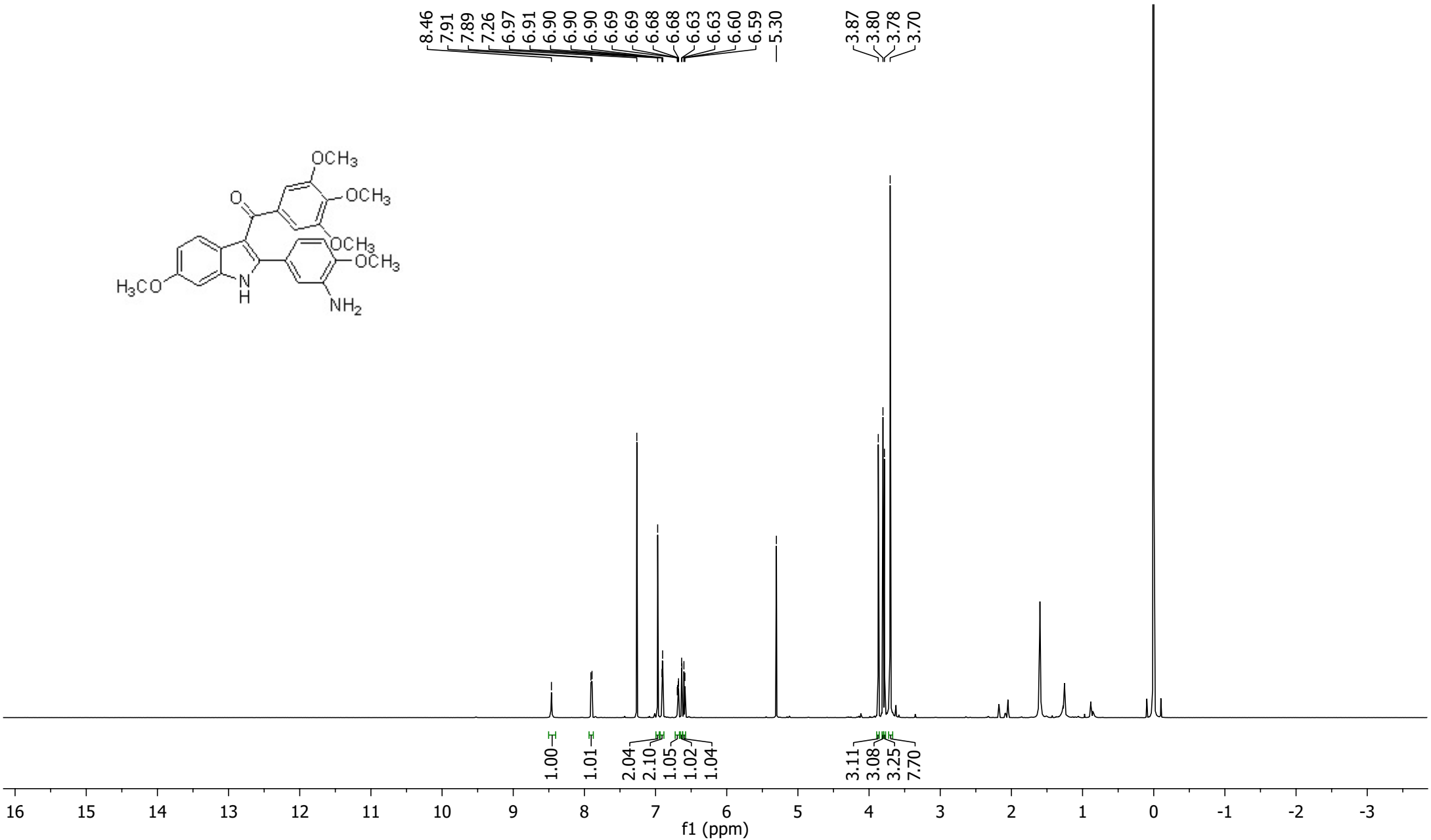

1H NMR (600 MHz) for Compound **5**

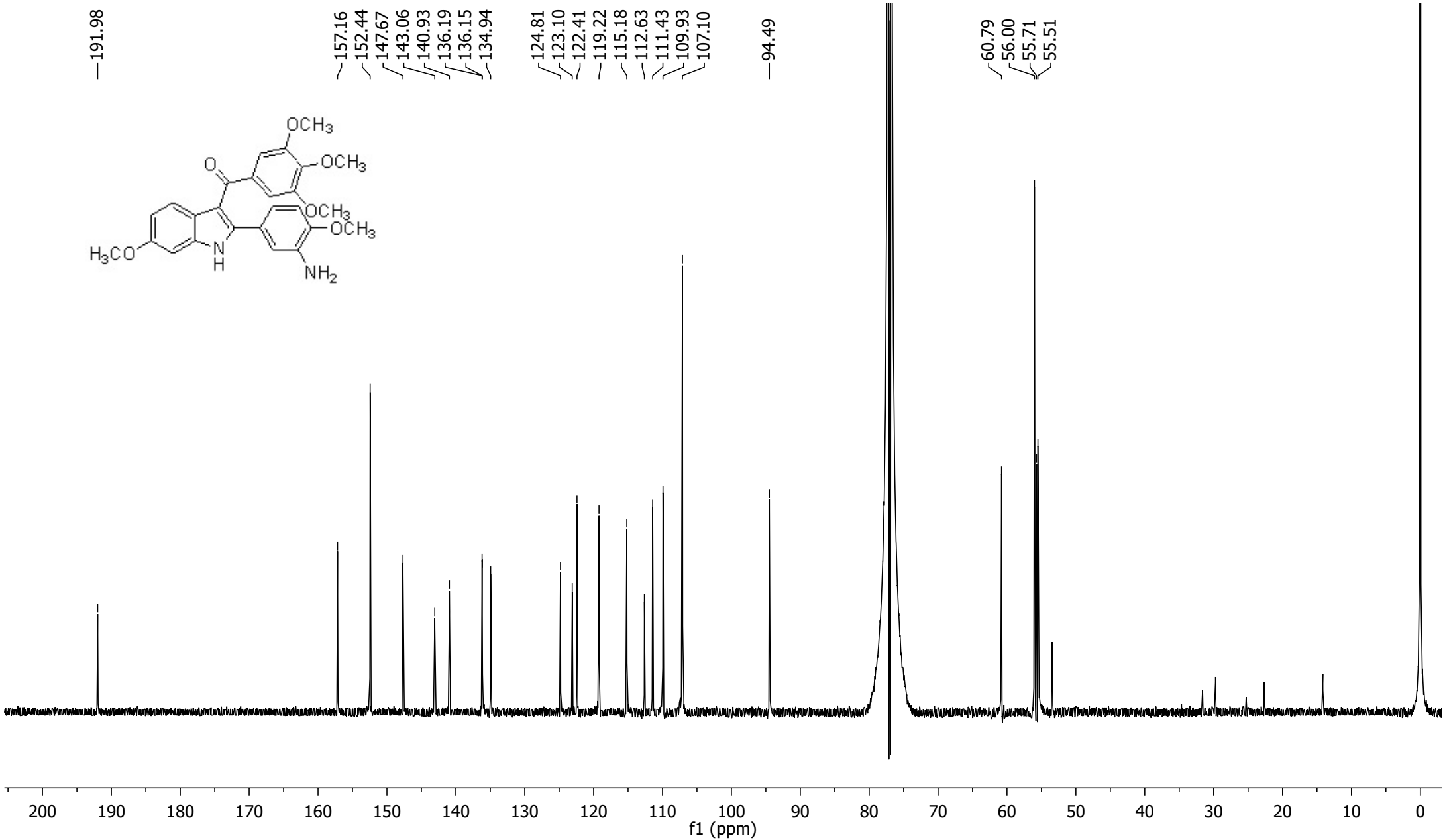

13C NMR (125 MHz) for Compound **5**

HRMS for Compound 5

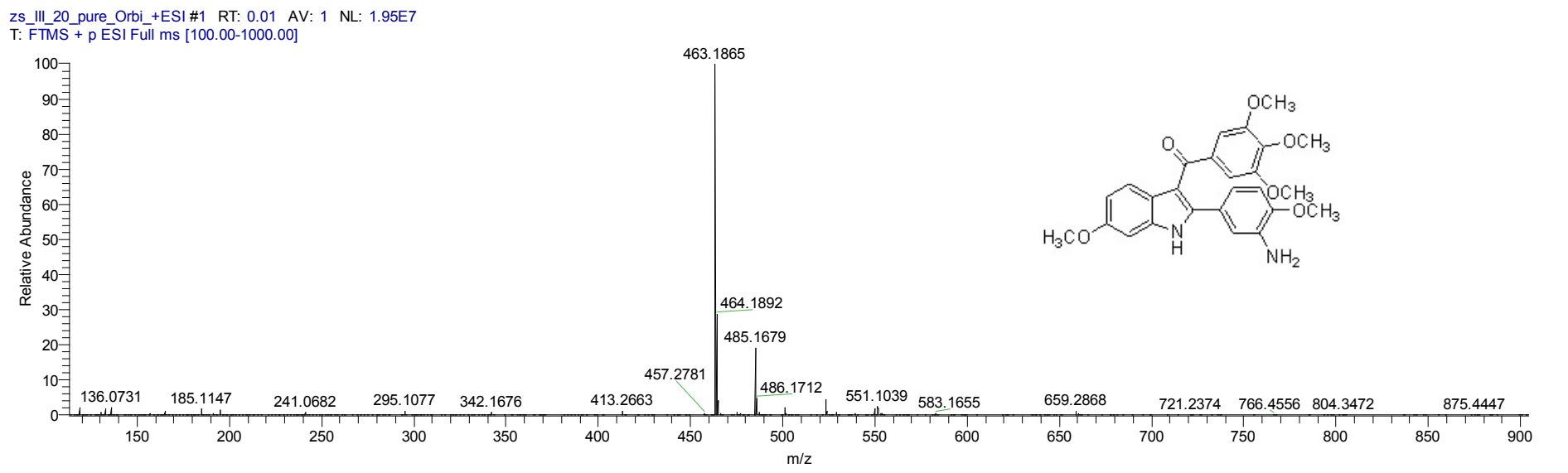

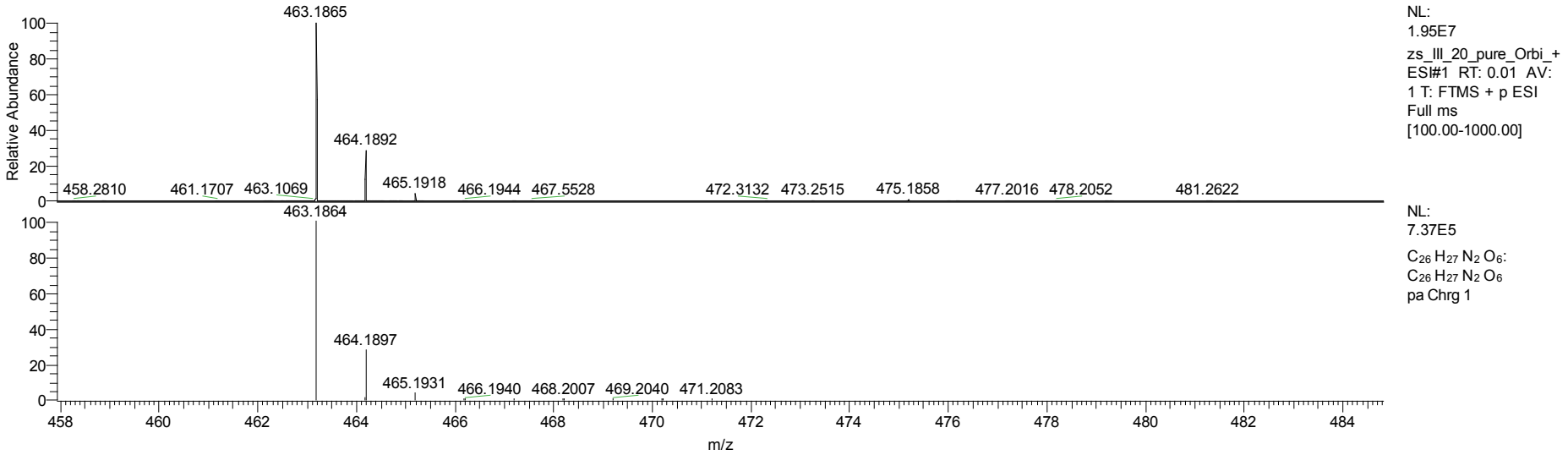

HPLC Trace for Compound 5

```
==========================================================================
Acq. Operator   : zhe
Acq. Instrument : Instrument 1                    Location :   -
Injection Date  : 7/25/2015 12:56:06 PM
Acq. Method     : C:\CHEM32\1\METHODS\GRAD 2 50-90 ACN.M
Last changed    : 7/25/2015 12:29:01 PM by zhe
Analysis Method : C:\CHEM32\1\DATA\ZHE\ZS_III_20000070.D\DA.M (GRAD 2 50-90 ACN.M)
Last changed    : 7/27/2015 6:04:01 PM by zhe
                  (modified after loading)
Sample Info     : zs_III_20
                  20150724
                  GRAD 2 50-90-ACN
```

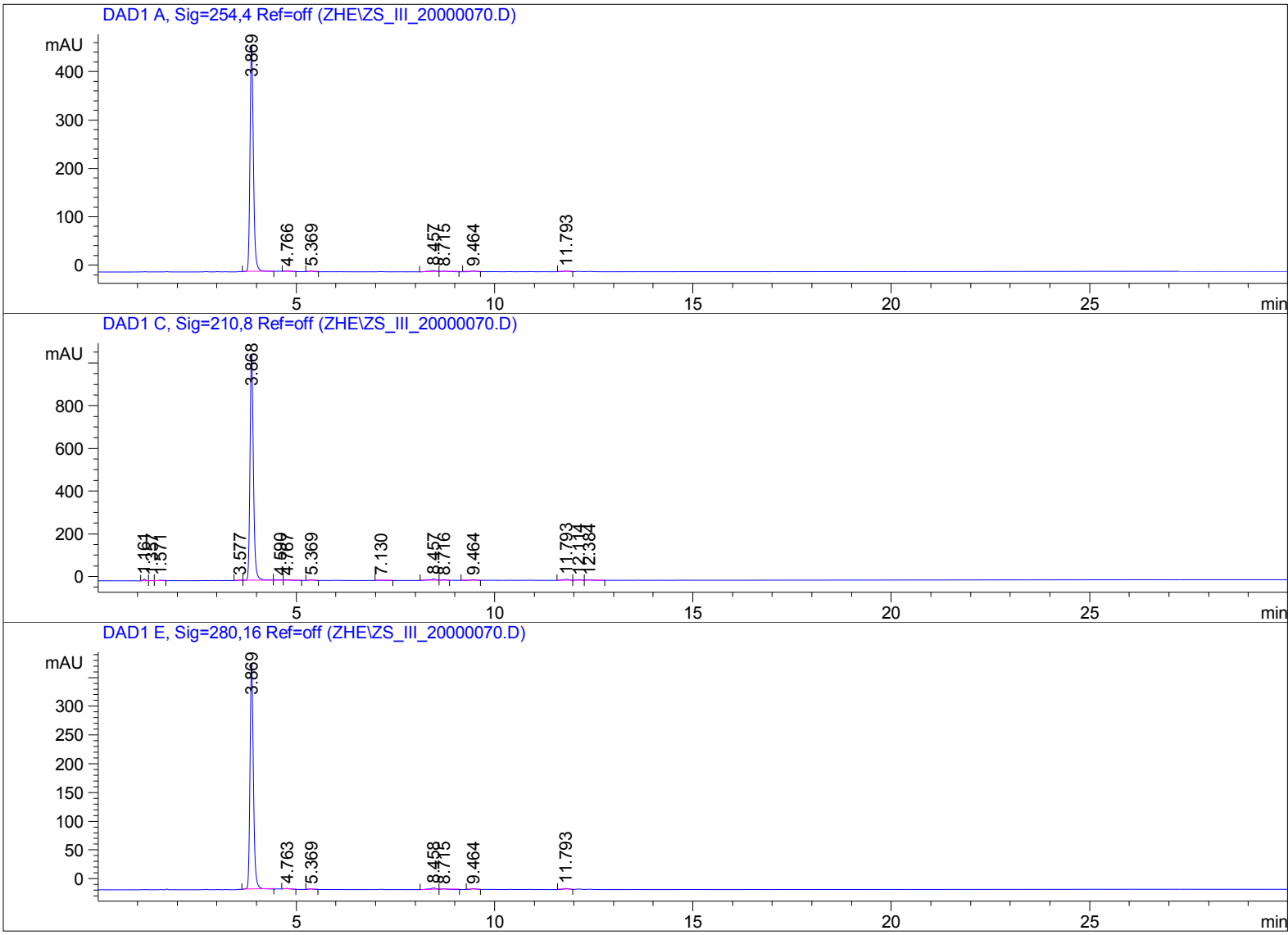

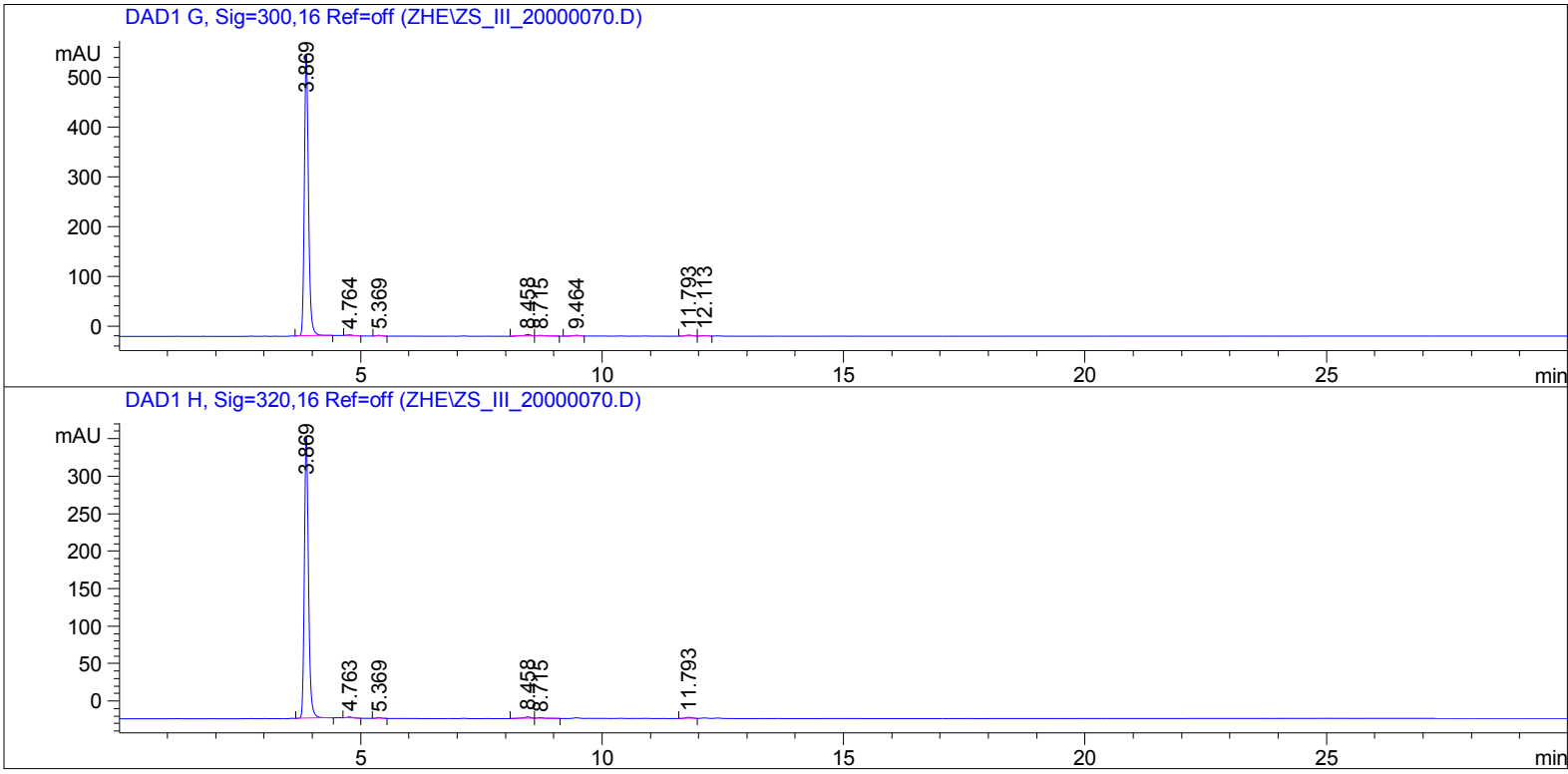

==========

Area Percent Report

==========

Sorted By : Signal
Multiplier : 1.0000
Dilution : 1.0000
Use Multiplier & Dilution Factor with ISTDs

Signal 1: DAD1 A, Sig=254,4 Ref=off

Peak #	RetTime [min]	Type	Width [min]	Area [mAU*s]	Height [mAU]	Area %
1	3.869	VB	0.0916	2789.46094	467.50934	96.7005
2	4.766	BB	0.1171	8.13293	1.06507	0.2819
3	5.369	BB	0.0997	10.08902	1.59808	0.3497
4	8.457	BV	0.1879	33.23231	2.51858	1.1520
5	8.715	VB	0.1742	15.83127	1.31772	0.5488
6	9.464	BB	0.1314	12.56040	1.50401	0.4354
7	11.793	BV	0.1583	15.33231	1.51223	0.5315
Totals :				2884.63916	477.02503	

Signal 2: DAD1 C, Sig=210,8 Ref=off

Peak #	RetTime [min]	Type	Width [min]	Area [mAU*s]	Height [mAU]	Area %
1	1.161	BV	0.0698	37.37536	8.10029	0.5545
2	1.357	VV	0.0859	9.20983	1.49339	0.1366
3	1.571	VB	0.0921	16.50322	2.46679	0.2448
4	3.577	BV	0.0958	16.30973	2.57912	0.2420
5	3.868	VV	0.0922	6366.70215	1058.72461	94.4546
6	4.590	VV	0.1760	35.69058	2.66880	0.5295
7	4.767	VB	0.1682	35.20403	2.92969	0.5223
8	5.369	BB	0.0992	18.45627	2.94114	0.2738
9	7.130	BB	0.1149	10.54125	1.41467	0.1564
10	8.457	BV	0.1781	70.04753	5.66962	1.0392
11	8.716	VB	0.1316	21.09575	2.52120	0.3130
12	9.464	BB	0.1308	21.97367	2.64869	0.3260
13	11.793	BV	0.1599	43.52880	4.23486	0.6458
14	12.114	VV	0.1592	21.63781	2.08365	0.3210
15	12.384	VB	0.1521	16.21356	1.60223	0.2405
Totals :				6740.48954	1102.07877	

Signal 3: DAD1 E, Sig=280,16 Ref=off

Peak #	RetTime [min]	Type	Width [min]	Area [mAU*s]	Height [mAU]	Area %
1	3.869	VB	0.0918	2353.67969	393.29330	96.1076
2	4.763	BB	0.1200	9.89361	1.25441	0.4040
3	5.369	BB	0.0988	7.14092	1.14457	0.2916
4	8.458	BV	0.1727	32.78903	2.75740	1.3389
5	8.715	VB	0.1674	16.66070	1.45664	0.6803
6	9.464	BB	0.1299	11.63528	1.41604	0.4751
7	11.793	BV	0.1556	17.20648	1.73628	0.7026
Totals :				2449.00571	403.05865	

Signal 4: DAD1 G, Sig=300,16 Ref=off

Peak #	RetTime [min]	Type	Width [min]	Area [mAU*s]	Height [mAU]	Area %
1	3.869	VB	0.0916	3370.28687	564.60181	96.3230
2	4.764	BB	0.1184	12.13207	1.56649	0.3467
3	5.369	BB	0.0989	9.79876	1.56792	0.2800
4	8.458	BV	0.1769	39.76372	3.24728	1.1364
5	8.715	VB	0.1706	20.17021	1.72250	0.5765

Peak #	RetTime [min]	Type	Width [min]	Area [mAU*s]	Height [mAU]	Area %
6	9.464	BB	0.1294	13.48599	1.64899	0.3854
7	11.793	BV	0.1599	22.07425	2.14790	0.6309
8	12.113	VV	0.1637	11.22981	1.07620	0.3209
Totals :				3498.94167	577.57908	

Signal 5: DAD1 H, Sig=320,16 Ref=off

Peak #	RetTime [min]	Type	Width [min]	Area [mAU*s]	Height [mAU]	Area %
1	3.869	BB	0.0917	2238.90576	374.76431	96.7496
2	4.763	BB	0.1198	10.62679	1.35125	0.4592
3	5.369	BB	0.0989	6.98290	1.11814	0.3018
4	8.458	BV	0.1718	26.70467	2.26045	1.1540
5	8.715	VB	0.1709	14.22055	1.21156	0.6145
6	11.793	BV	0.1591	16.68314	1.63365	0.7209
Totals :				2314.12381	382.33936	

==========

*** End of Report ***

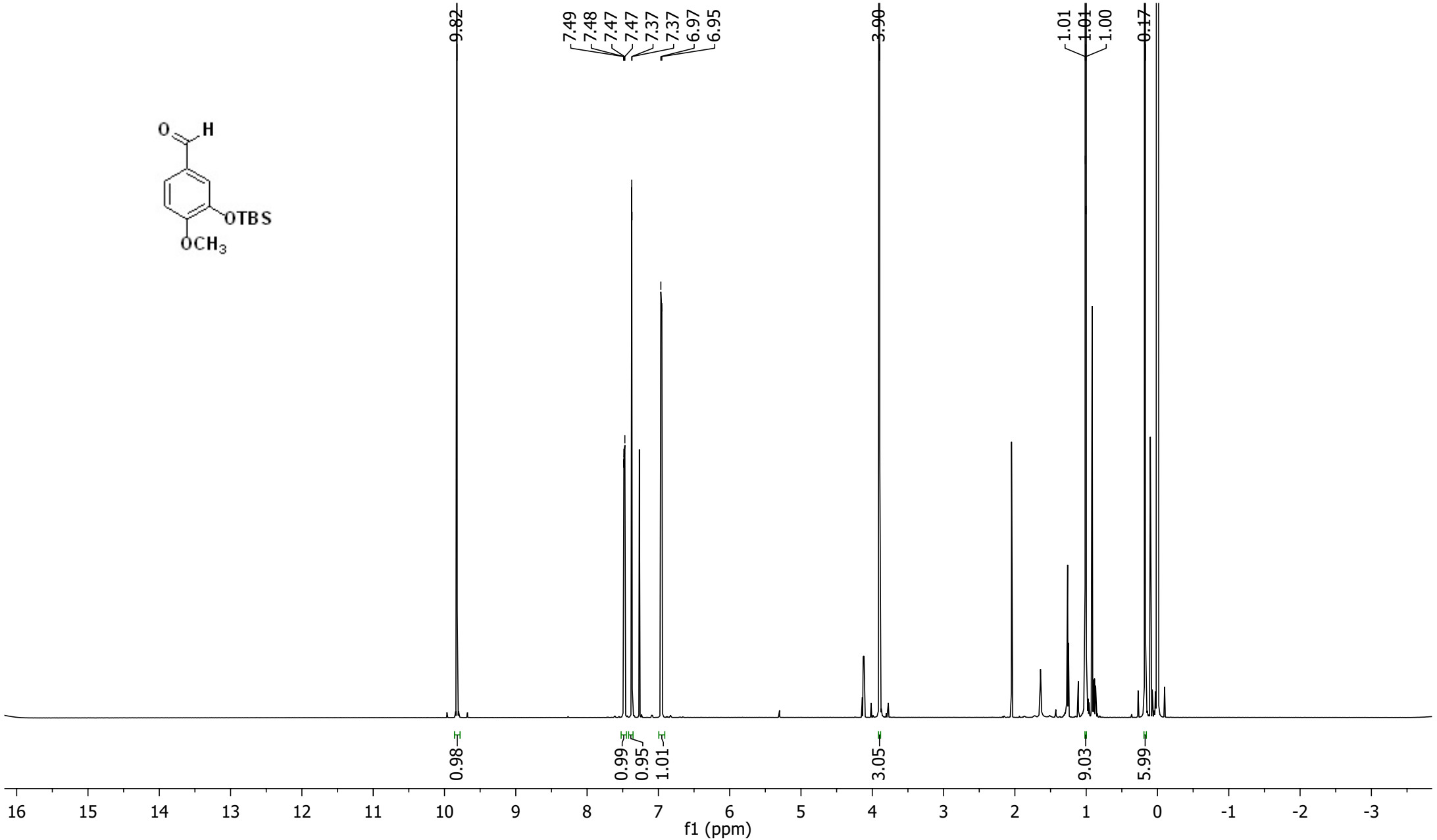

1H NMR (600 MHz) for Compound **7**

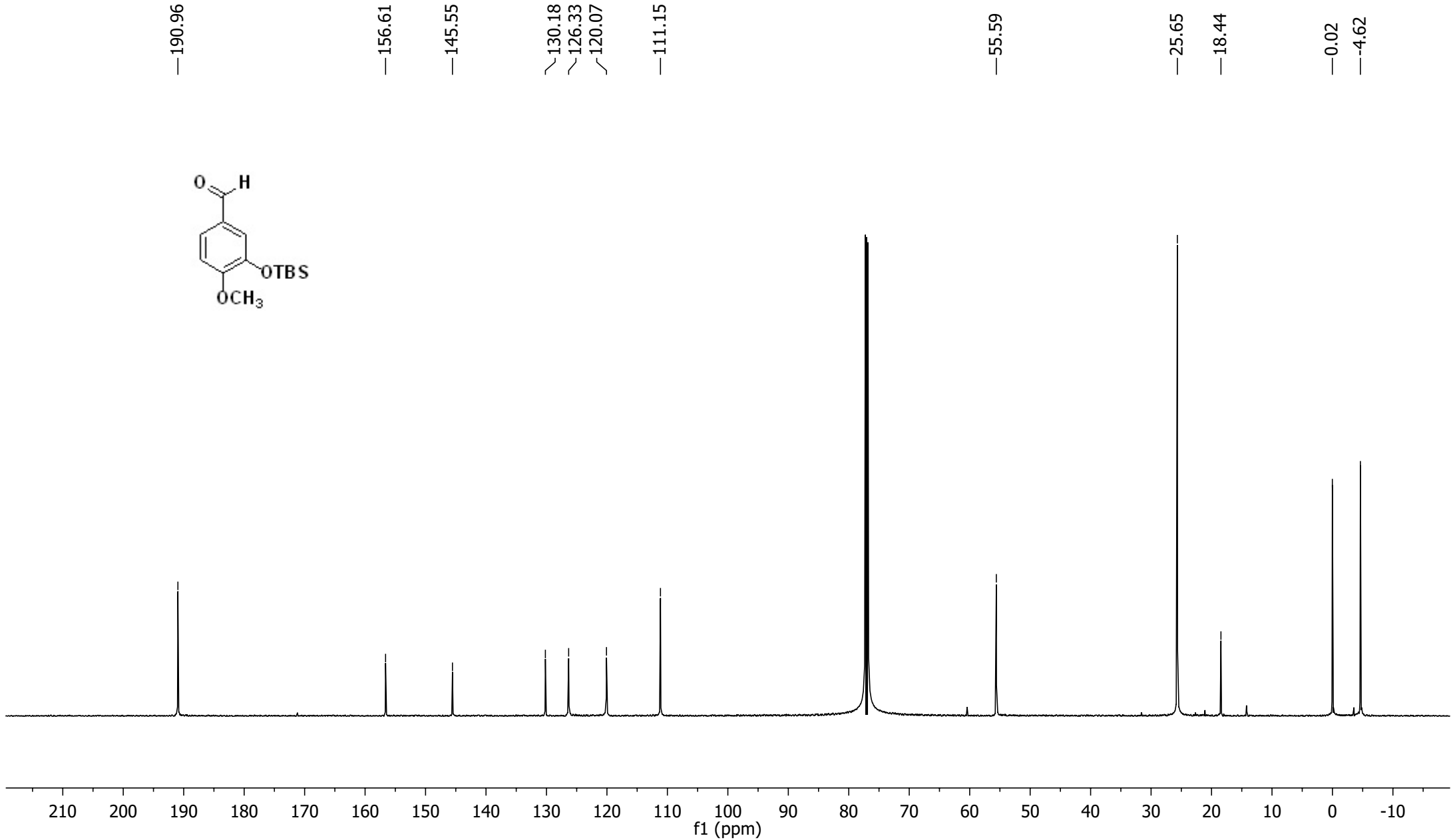

13C NMR (125 MHz) for Compound **7**

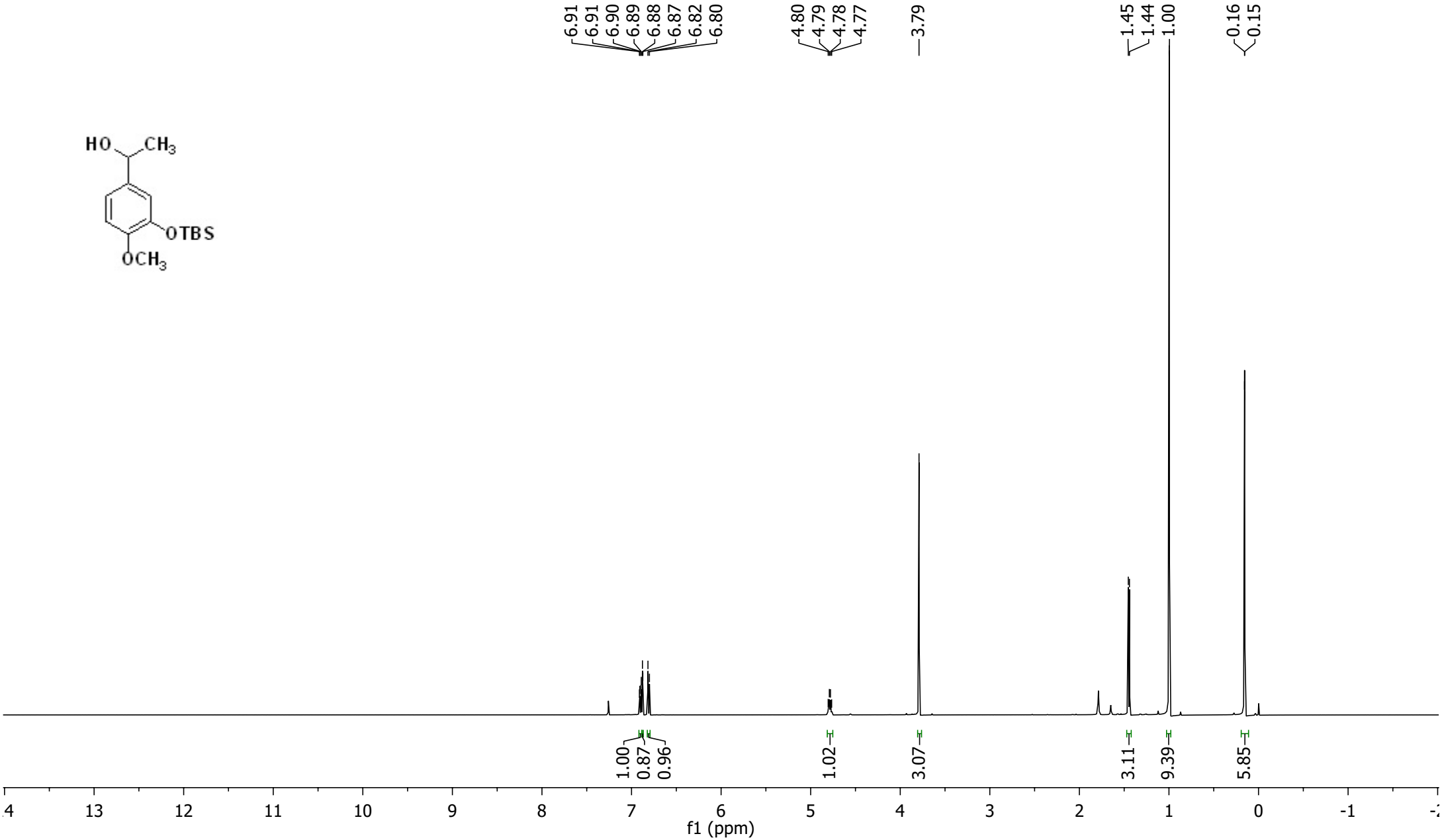

1H NMR (600 MHz) for Compound **8**

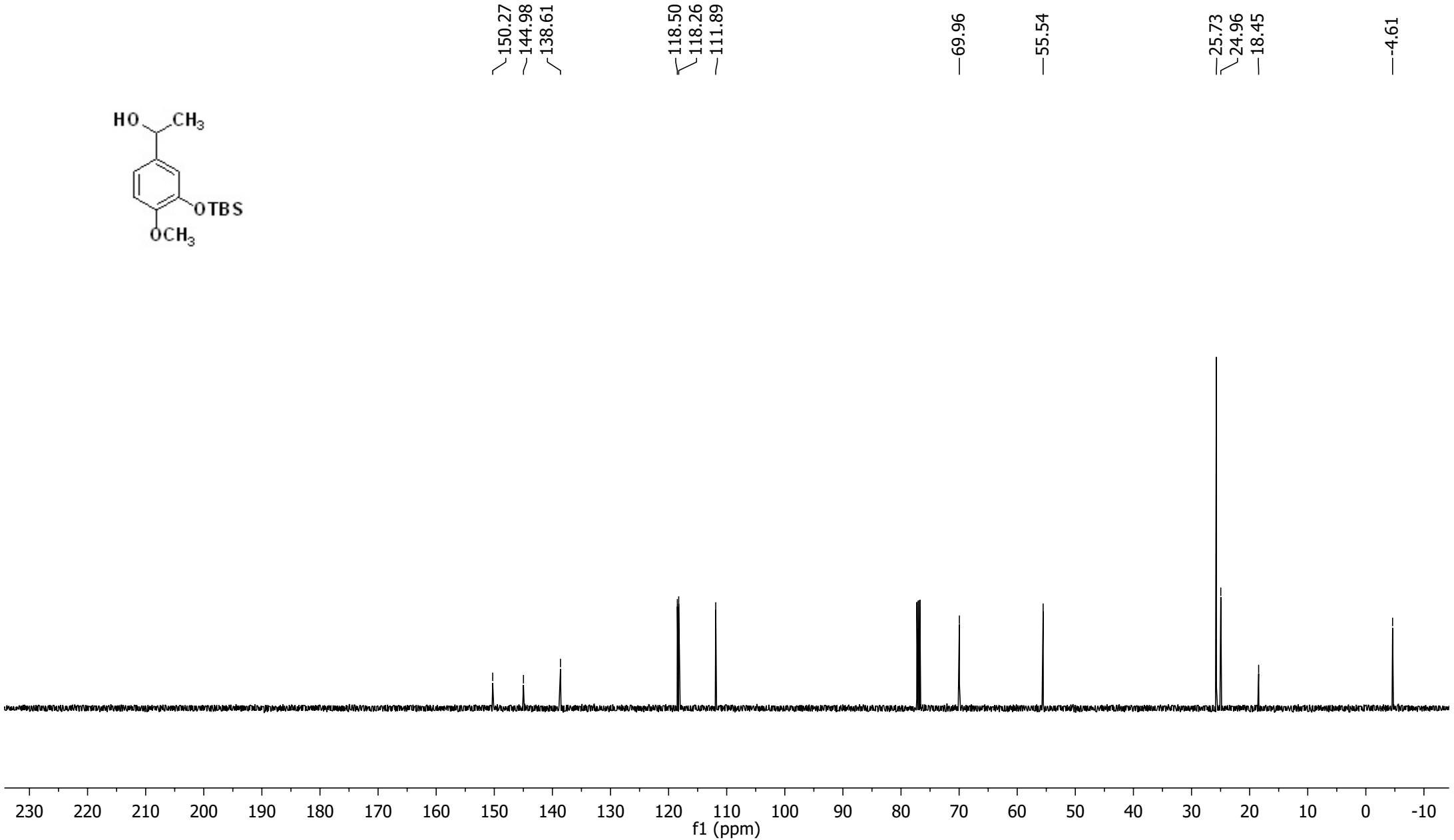

13C NMR (125 MHz) for Compound **8**

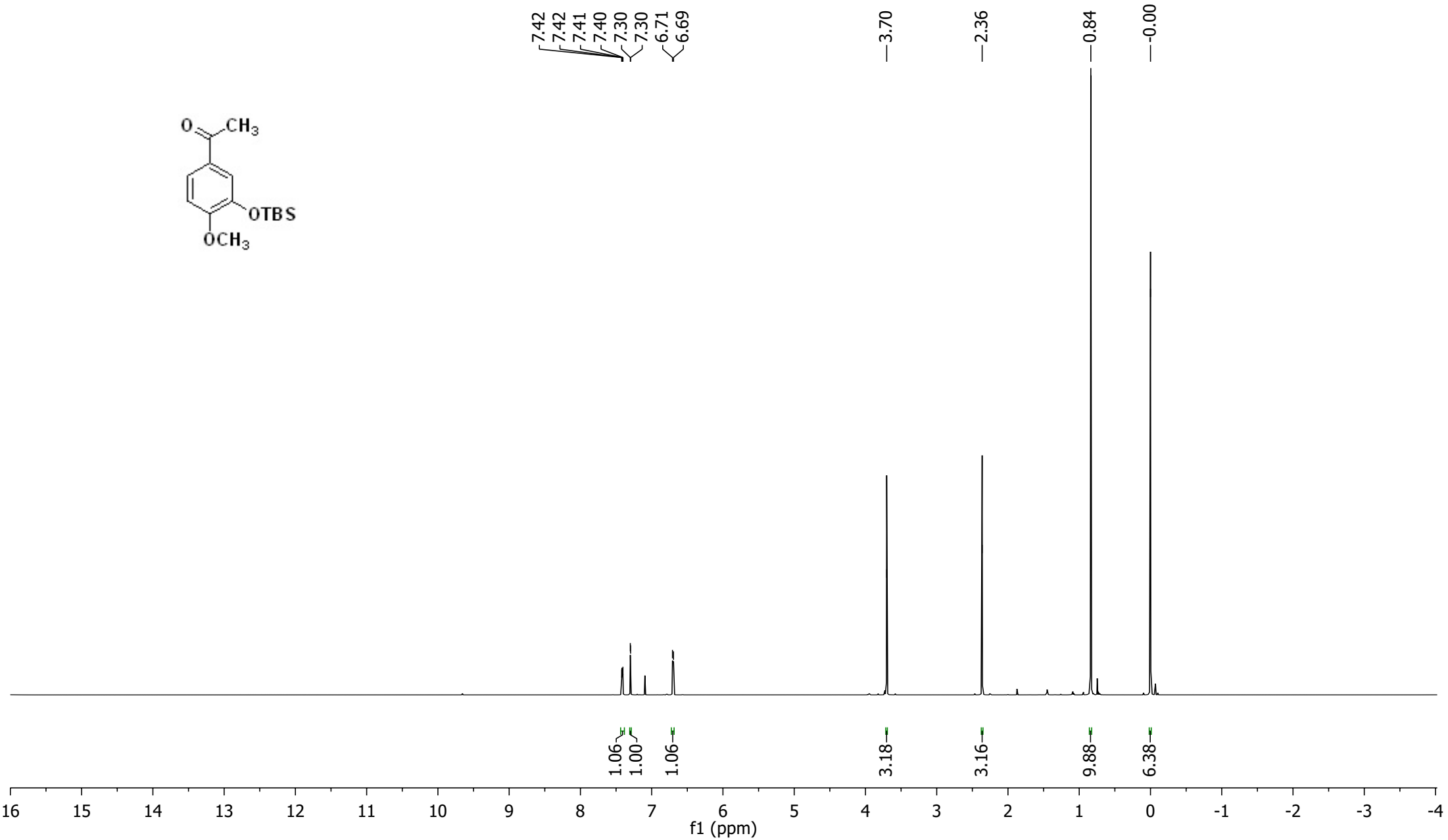

1H NMR (600 MHz) for Compound 9

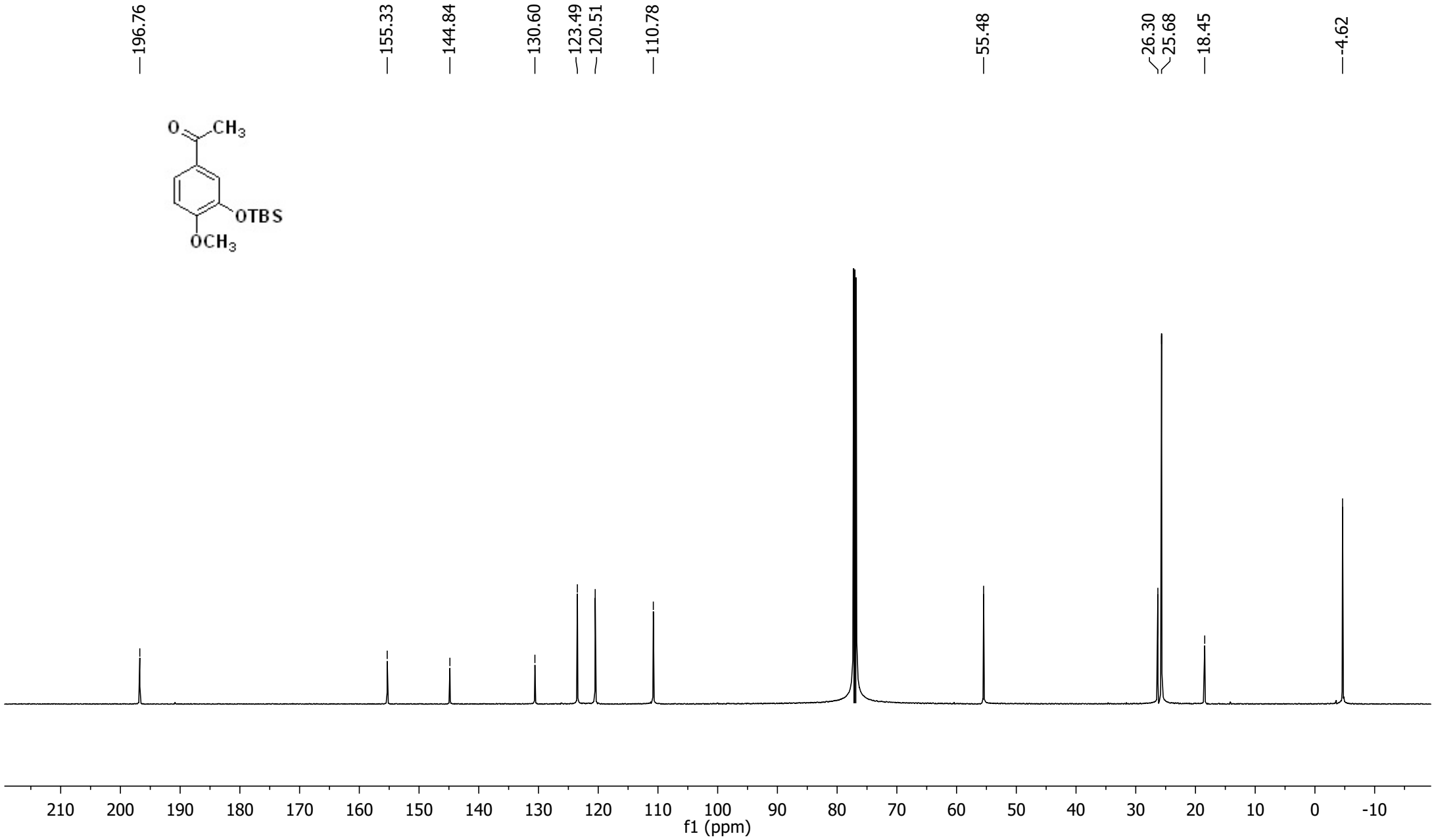

13C NMR (125 MHz) for Compound 9

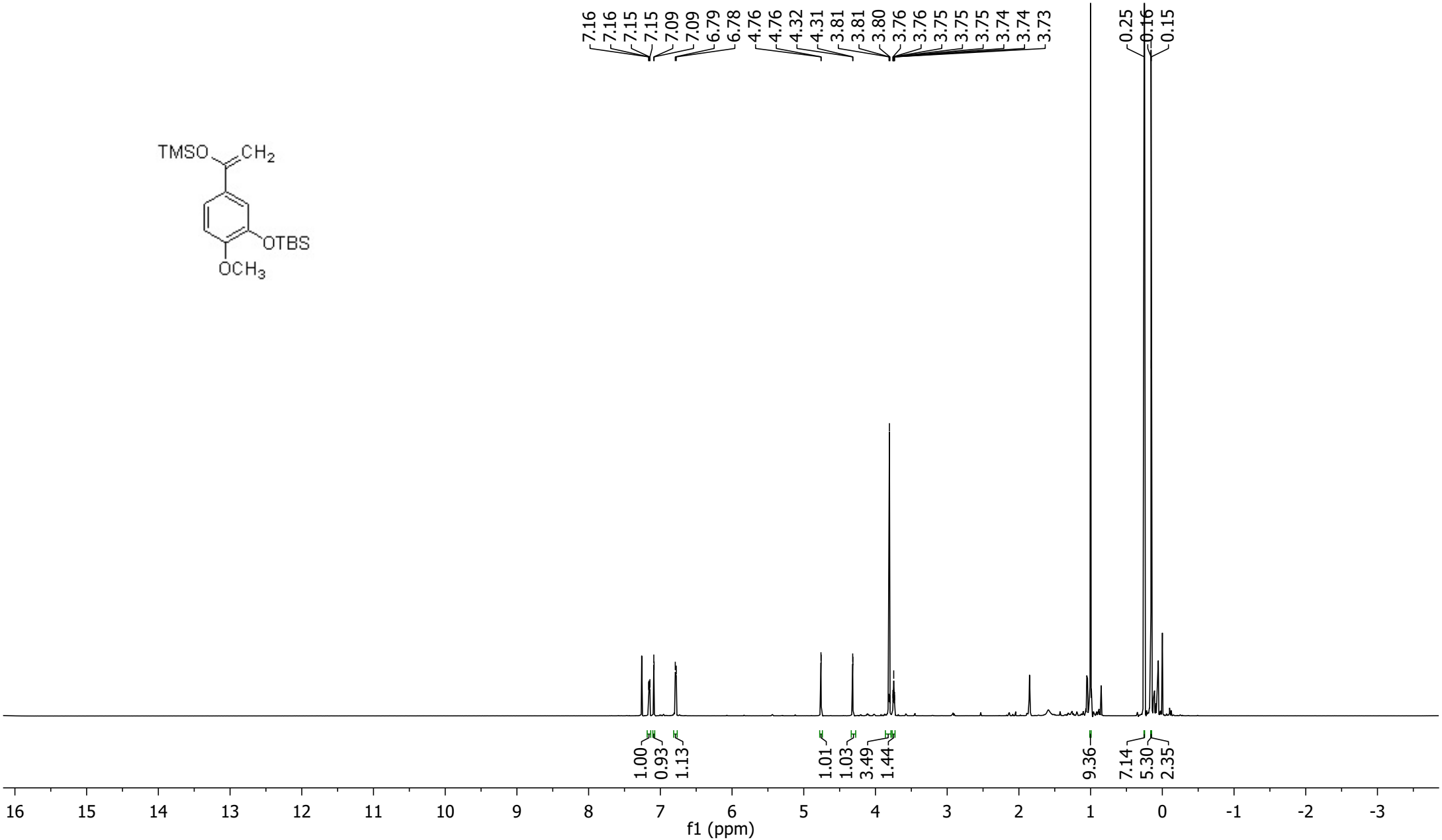

1H NMR (600 MHz) for Compound **10**

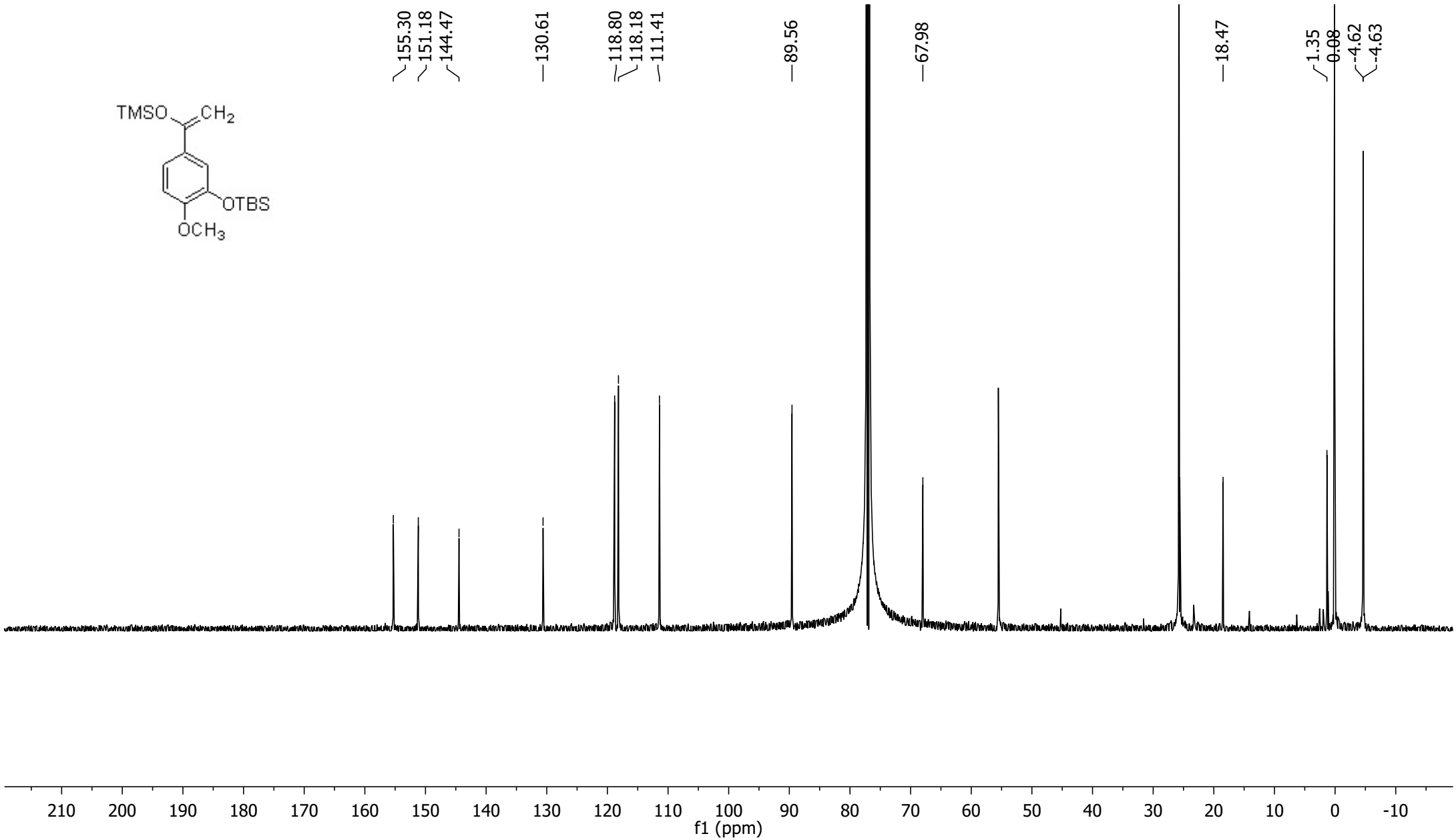

13C NMR (125 MHz) for Compound **10**

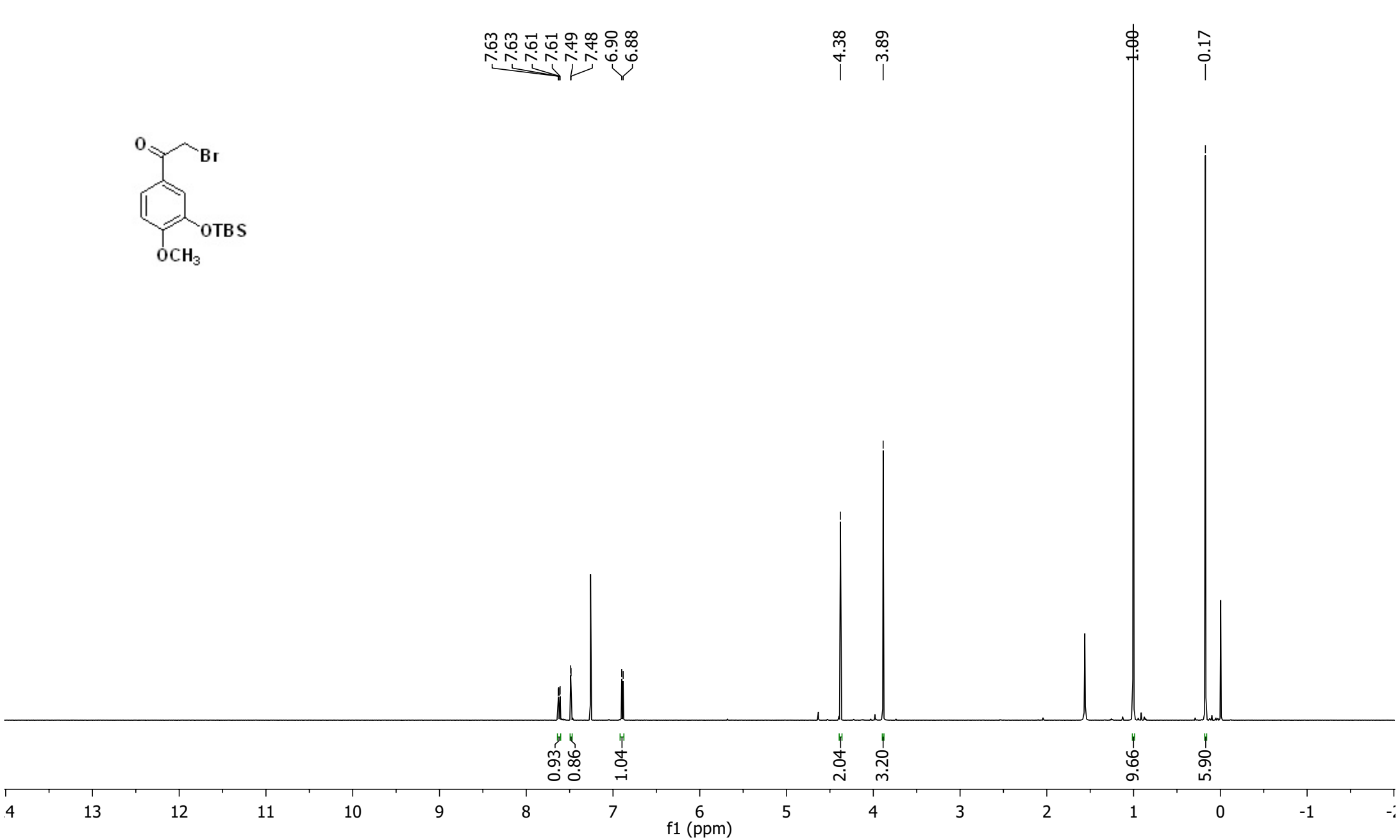

1H NMR (600 MHz) for Compound **11**

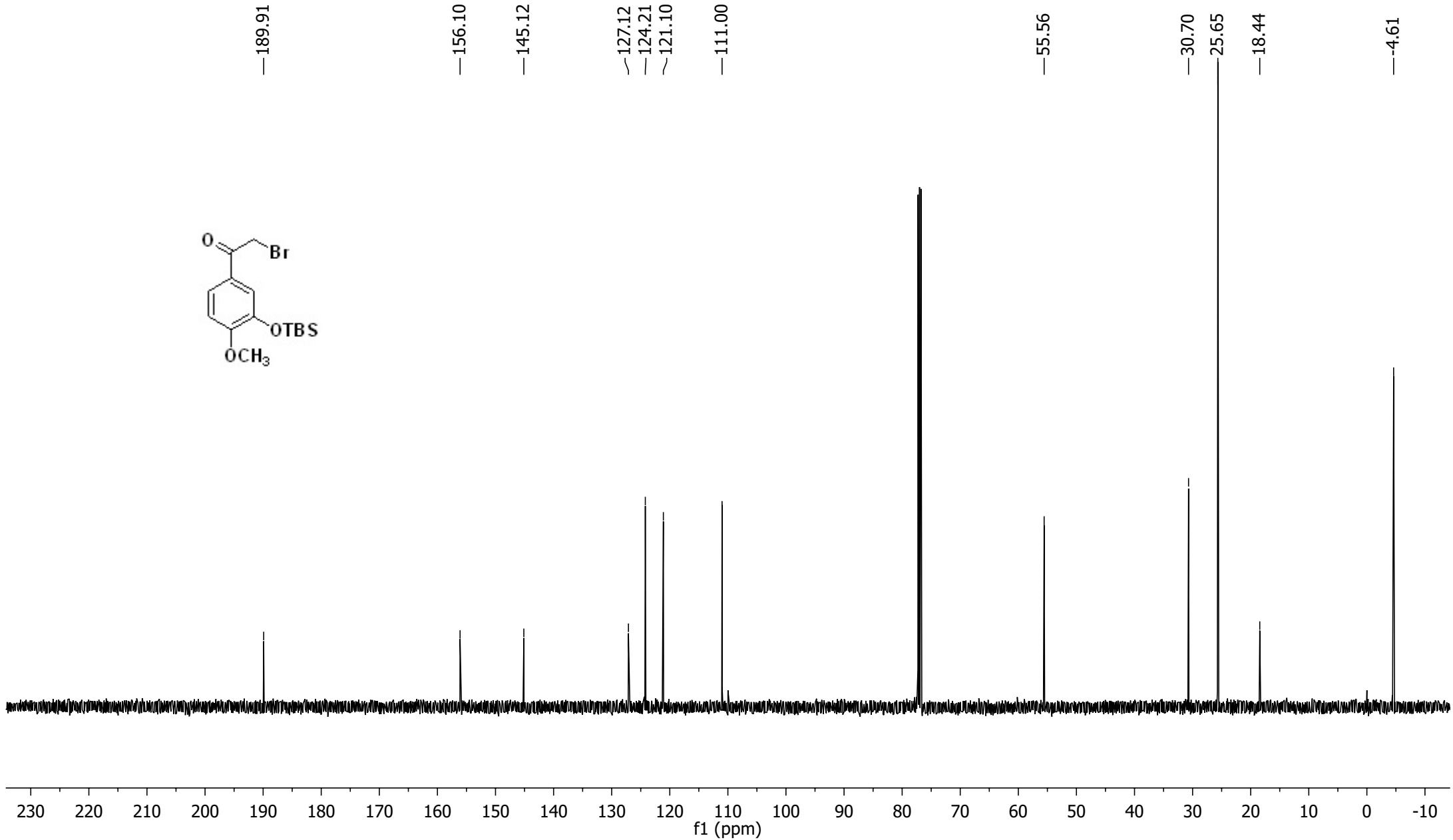

13C NMR (125 MHz) for Compound **11**

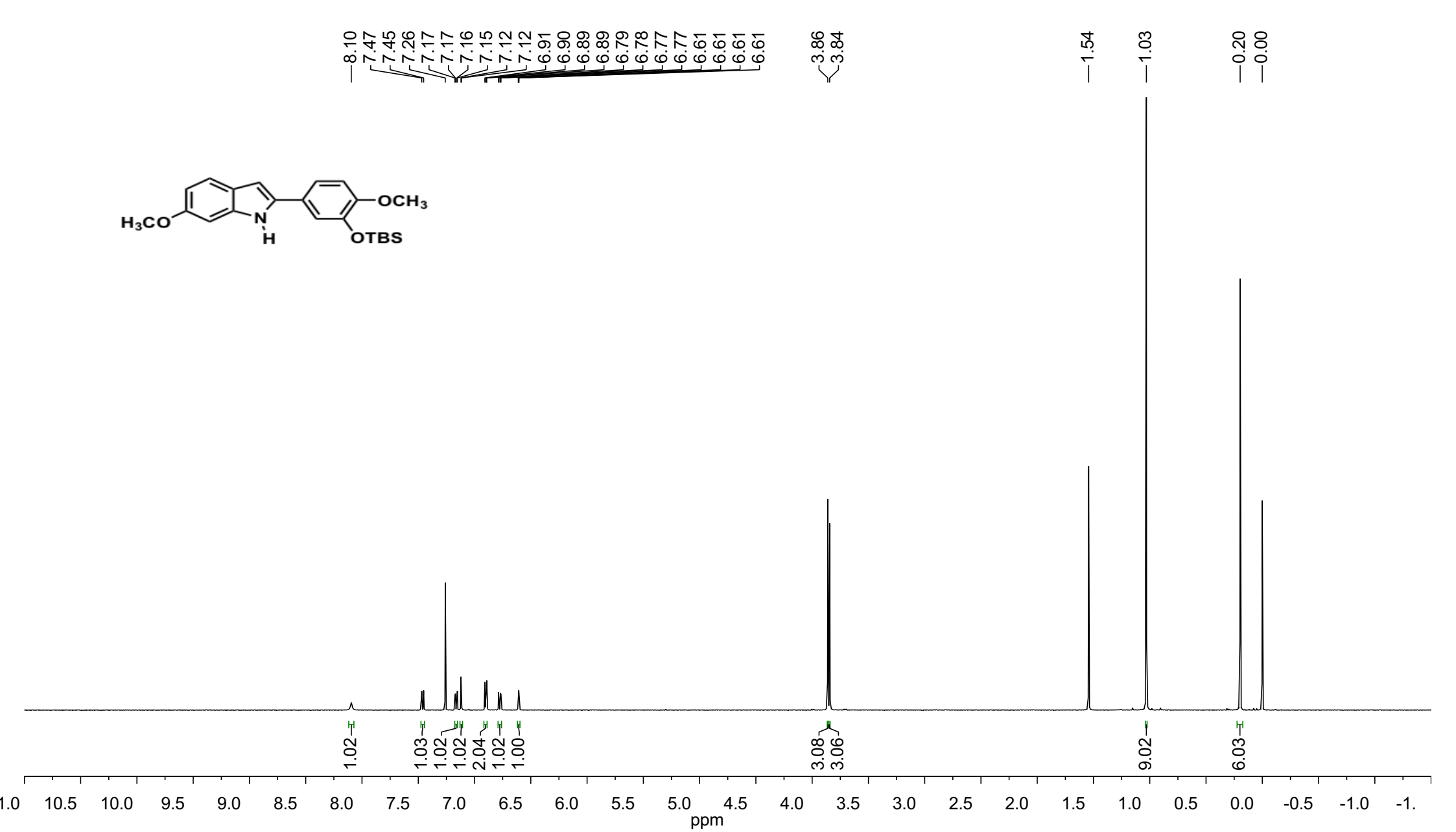

1H NMR (600 MHz) for Compound 12

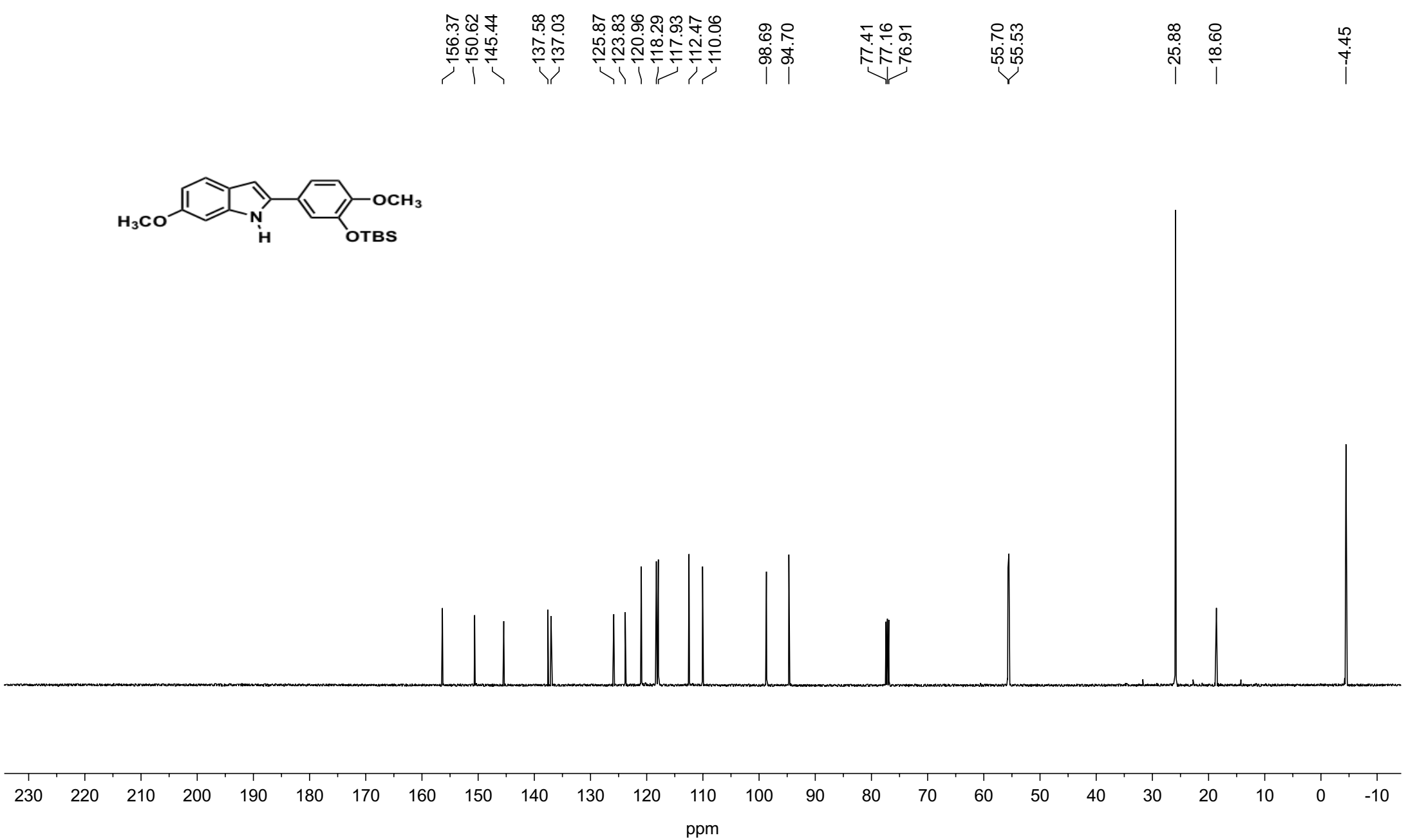

13C NMR (125 MHz) for Compound 12

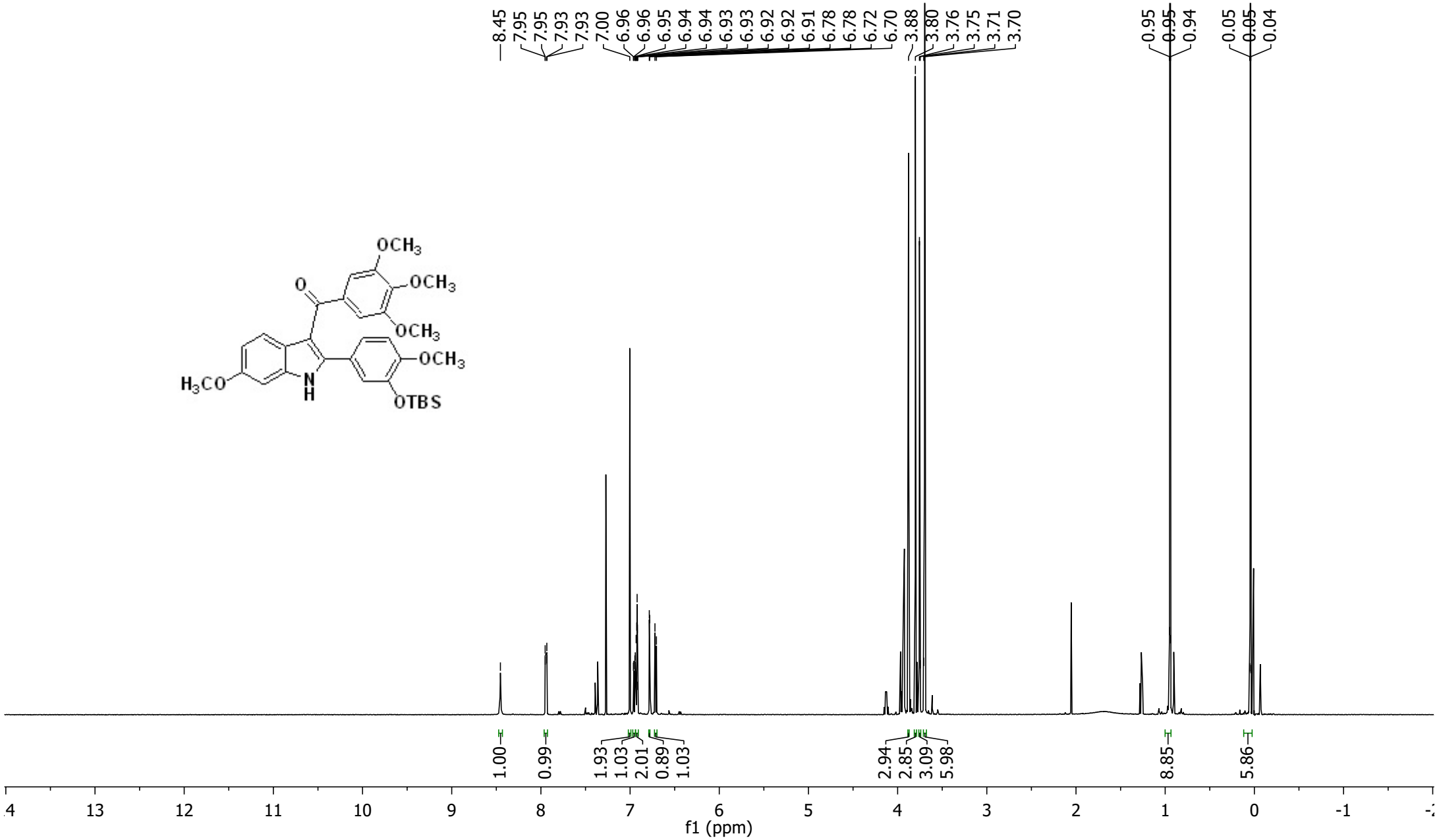

1H NMR (600 MHz) for Compound **13**

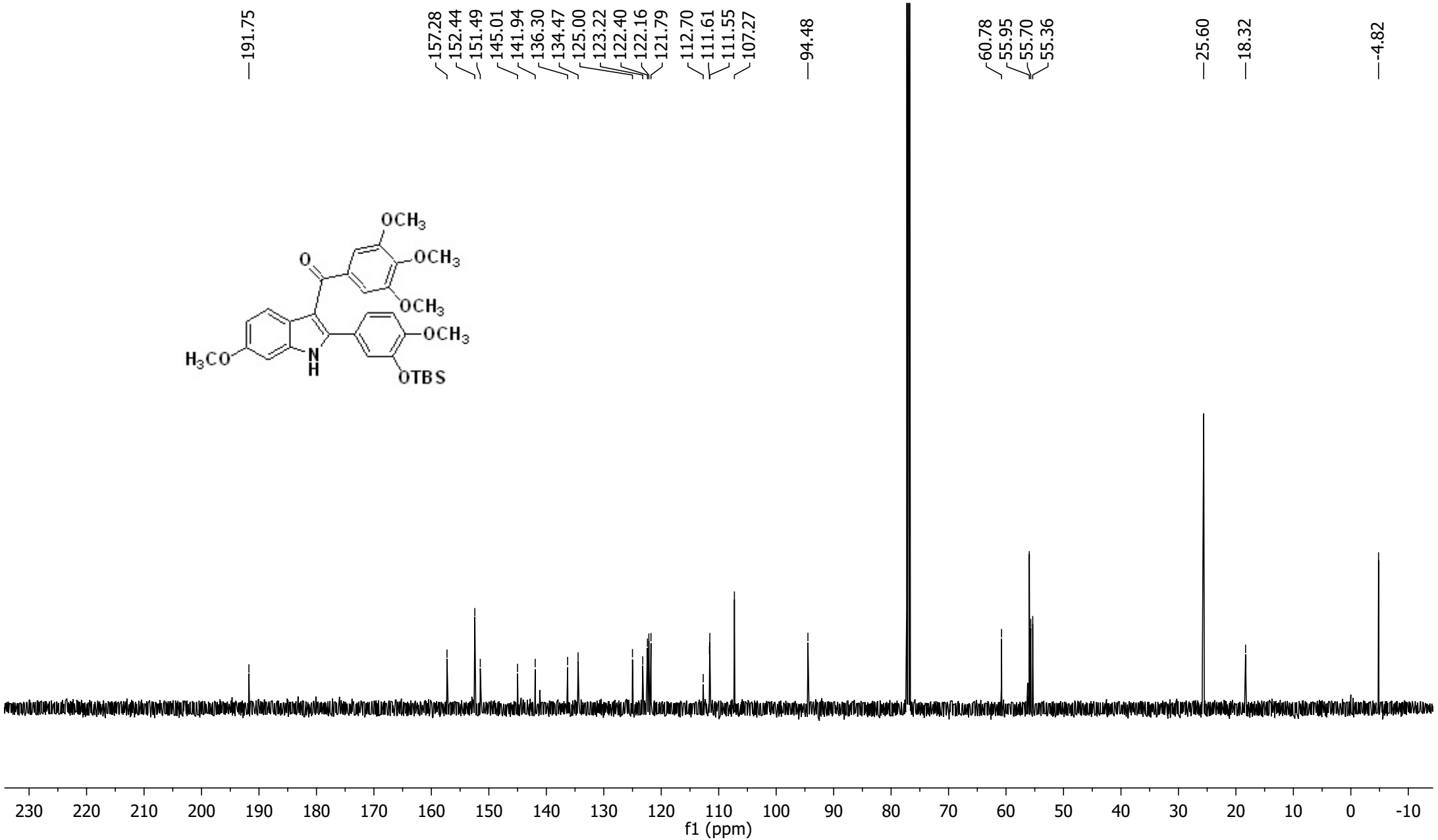

13C NMR (125 MHz) for Compound **13**

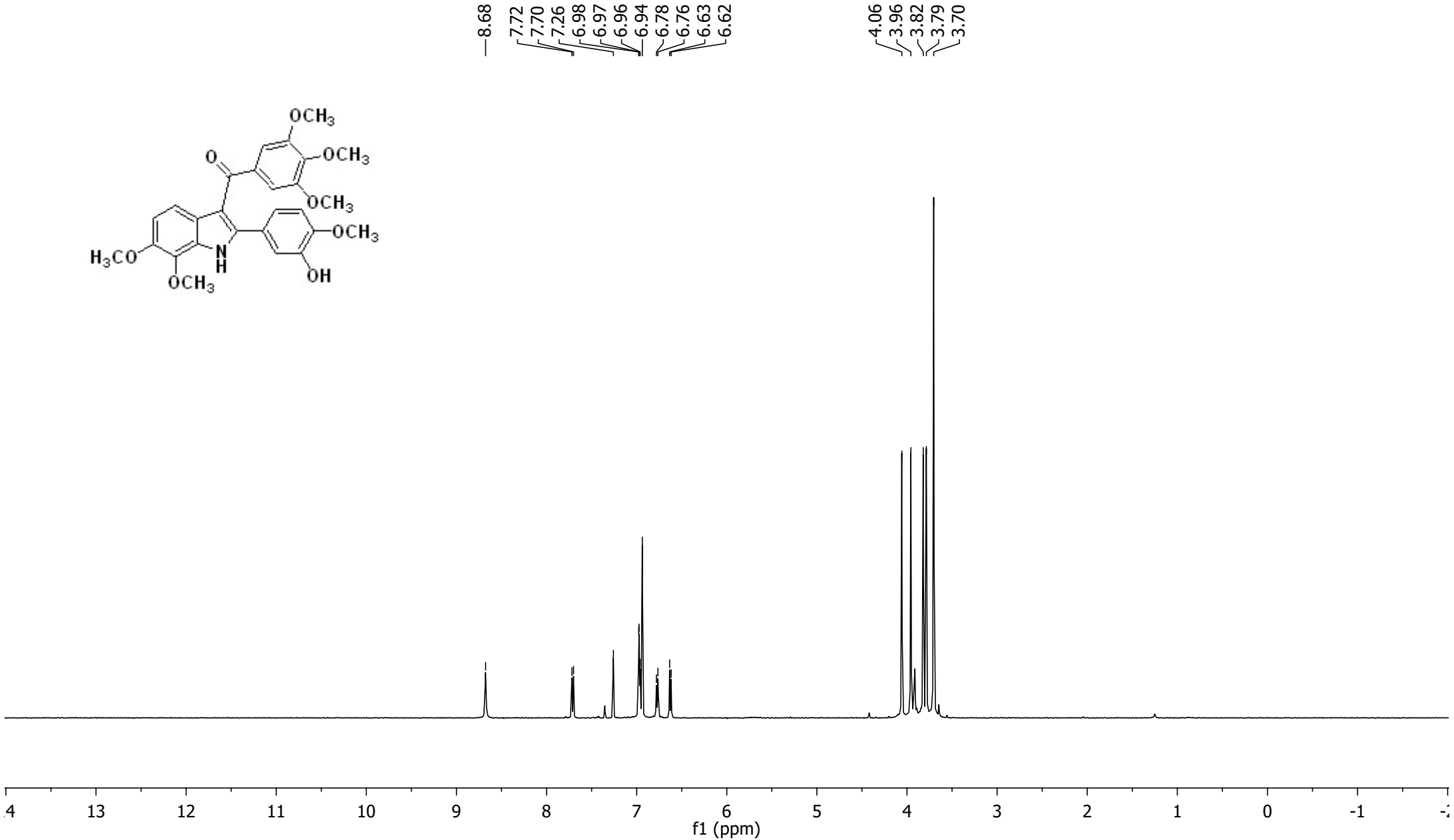

1H NMR (600 MHz) for Compound **14**

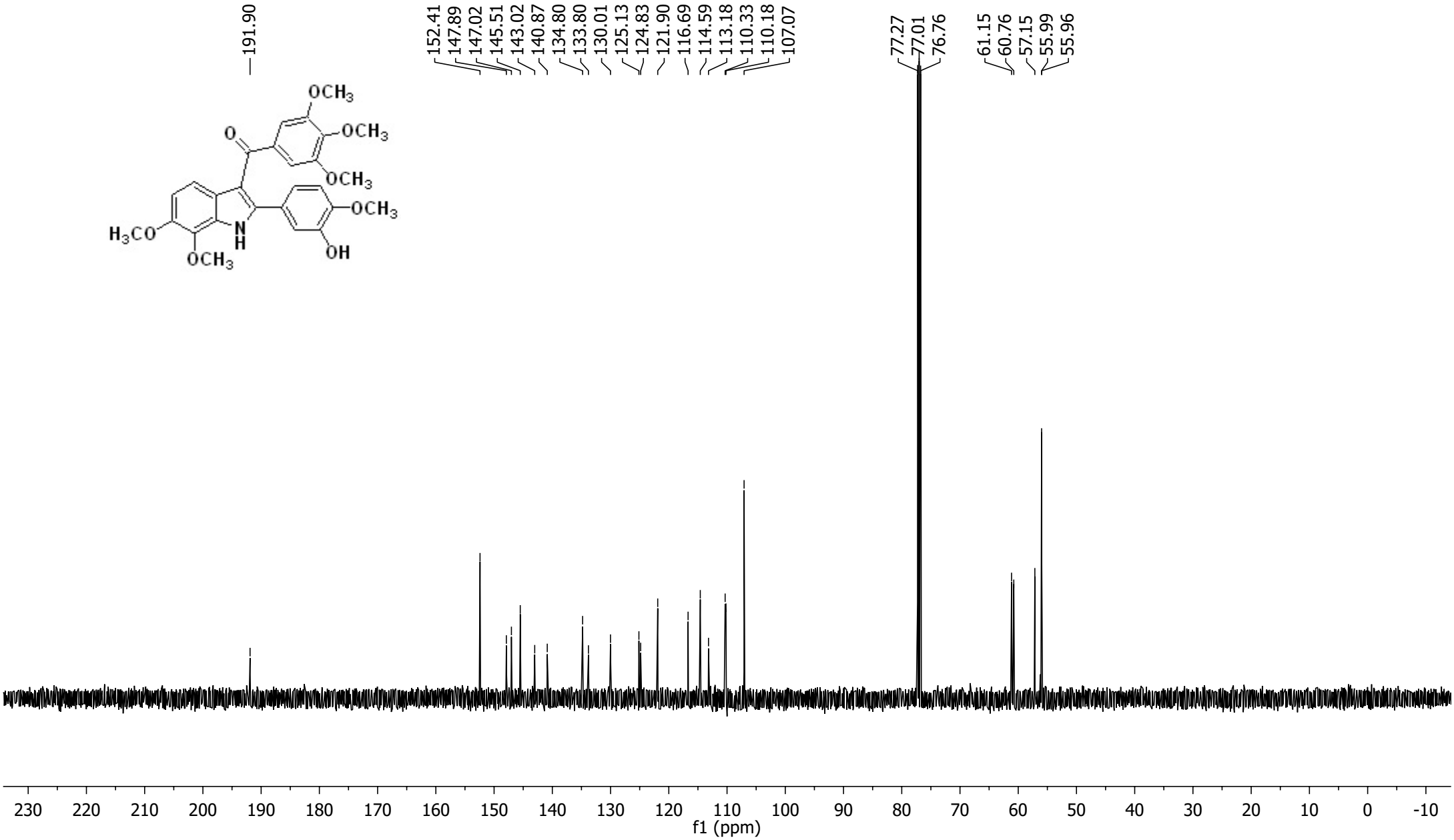

13C NMR (125 MHz) for Compound **14**